Accepted Article Preview: Published ahead of online publication

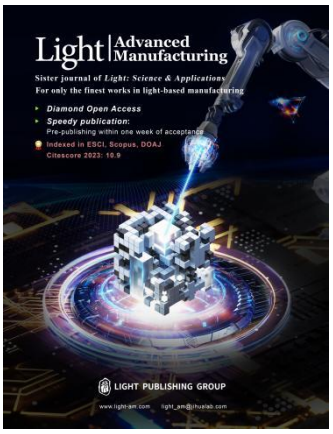

Optical Manufacturing and Testing of Large -Aperture Optical Mirrors: A Review

Longxiang Li, Xuejun Zhang, Qiang Cheng, Donglin Xue, Ximing Liu, Yunfan Yang, Hongshi Li, Runmu Cheng

Cite this article as: Longxiang Li, Xuejun Zhang, Qiang Cheng, Donglin Xue, Ximing Liu, Yunfan Yang, Hongshi Li, Runmu Cheng. Optical Manufacturing and Testing of Large-Aperture Optical Mirrors: A Review. *Light: Advanced Manufacturing* accepted article preview 22 June, 2026; doi: 10.37188/lam.2026.104

Received 11 August 2025; Revised 18 June 2026; Accepted 22 June 2026;
Accepted article preview online 22 June 2026

Optical Manufacturing and Testing of Large-Aperture Optical Mirrors: A Review

Longxiang Li[1,2,3], Xuejun Zhang[1,2,3, *], Qiang Cheng[1,2,3], Donglin Xue[1,2,3], Ximing Liu[1,2,3], Yunfan Yang[1,2,3], Hongshi Li[1,2,3], Runmu Cheng[1,2,3],

[1] Changchun Institute of Optics, Fine Mechanics and Physics, Chinese Academy of Sciences, Changchun, 130033, China

[2] University of Chinese Academy of Sciences, Beijing 100049, China

[3] State Key Laboratory of Advanced Manufacturing for Optical System, China

*zxj@ciomp.ac.cn

Abstract

Large-aperture telescopes are indispensable tools for astronomical research. Over the past few decades, a host of representative projects have been developed, whose performance relies heavily on the manufacturing and testing technologies for large-aperture mirrors. This paper reviews the state-of-the-art fabrication and testing methods for large optical mirrors and is structured into five parts: application background, classification of manufacturing techniques, overview of metrology technologies, verification and standards, as well as conclusions and future perspectives. Sustained innovation in fabrication and testing lays a solid foundation for technological progress in this field and the implementation of next-generation telescope projects. Key development directions include achieving sub-nanometer-level surface accuracy, boosting large-batch manufacturing efficiency, upgrading metrology equipment and methodologies, and promoting the intelligent and automated integration in fabrication and metrology systems. It is expected that this review will serve as a valuable reference for researchers aiming to gain a full insight into understanding of manufacturing and testing technologies for large-aperture optical components.

Keywords: Large-aperture telescope, Optical fabrication, Optical testing

1. Introduction

Large-aperture telescopes serve as critical enabling technologies for a broad spectrum of applications, including astronomical observation, space science, Earth observation, exoplanet detection, gravitational-wave counterpart searches, environmental monitoring, disaster early warning, high-resolution imaging, and spectral analysis. Driven by these diverse demands, major international roadmaps and research programs have continued to promote the construction of advanced observation facilities and the development of next-generation telescope technologies.

The realization of these scientific missions depends strongly on advances in precision optical manufacturing and testing. Large-aperture optical mirrors must simultaneously meet demanding requirements in aspects such as aperture, surface figure accuracy, surface roughness, thermal stability, structural lightweight, and support accuracy. Their manufacturing therefore requires a coordinated technology chain: after the structural design and mirror blank preparation are completed, finer surface processing is carried out. In this process, surface figure error testing and geometric measurement iteratively guide and constrain manufacturing continuously to converge errors to meet high-precision surface figure standards before final acceptance.

Over the past several decades, numerous manufacturing and testing schemes have been implemented in major telescope projects worldwide. Manufacturing technologies such as computer-controlled optical surfacing, stressed-lap grinding/polishing, bonnet polishing, magnetorheological finishing (MRF), and ion beam figuring (IBF) and so on, have been widely used to improve surface figure accuracy and the efficiency of error correction during manufacturing. As iterative manufacturing progressively improves optical surface accuracy, the corresponding surface figure error detection and geometric measurements transition from high-dynamic-range profilometry at the early stage to nanometer-level wavefront sensing at the final stage. Commonly employed measurement techniques throughout

this process include laser tracking, Shack–Hartmann sensing, sub-aperture stitching interferometry, and computer-generated hologram (CGH) null testing, among others. This review focuses on the manufacturing and testing technologies of large-aperture optical mirrors, with emphasis on representative telescope projects and large optical components. The Hubble Space Telescope stands as an early space telescope milestone where the demand for ultra-high surface accuracy and complex freeform metrology in an unrepairable space environment drove revolutionary breakthroughs in manufacturing and testing. Therefore, on one hand, the aperture of monolithic mirrors has continued to increase to meet growing observational demands; on the other hand, segmented mirror technology has also evolved to enable even larger apertures. Based on these representative large-aperture manufacturing cases, this review synthesizes the current technical routes, compares their advantages and limitations, and discusses their applicability to future optical systems.

Fig. 1 presents the overall framework of this review, which proceeds from application requirements to manufacturing methods, testing technologies, performance evaluation, and future outlook. Following the Introduction, Section 2 introduces the application background of large-aperture optical mirrors in ground-based and space-based observation systems. Section 3 reviews the manufacturing process of large-aperture optical mirrors, beginning with an overview of the general fabrication flow, mirror structural configurations, and key manufacturing specifications. It then surveys typical processing techniques applicable to large-aperture mirrors, organized under the categories of monolithic primary mirrors and segmented mirrors. Section 4 discusses optical testing and metrology methods used during fabrication, covering rough-stage measurement, polishing-stage testing, null and non-null testing, and segmented-mirror alignment. Section 5 summarizes key performance parameters and acceptance criteria, linking manufacturing capability with system-level optical requirements. Finally, Section 6 presents the summary and outlook, highlighting current challenges and future research directions.

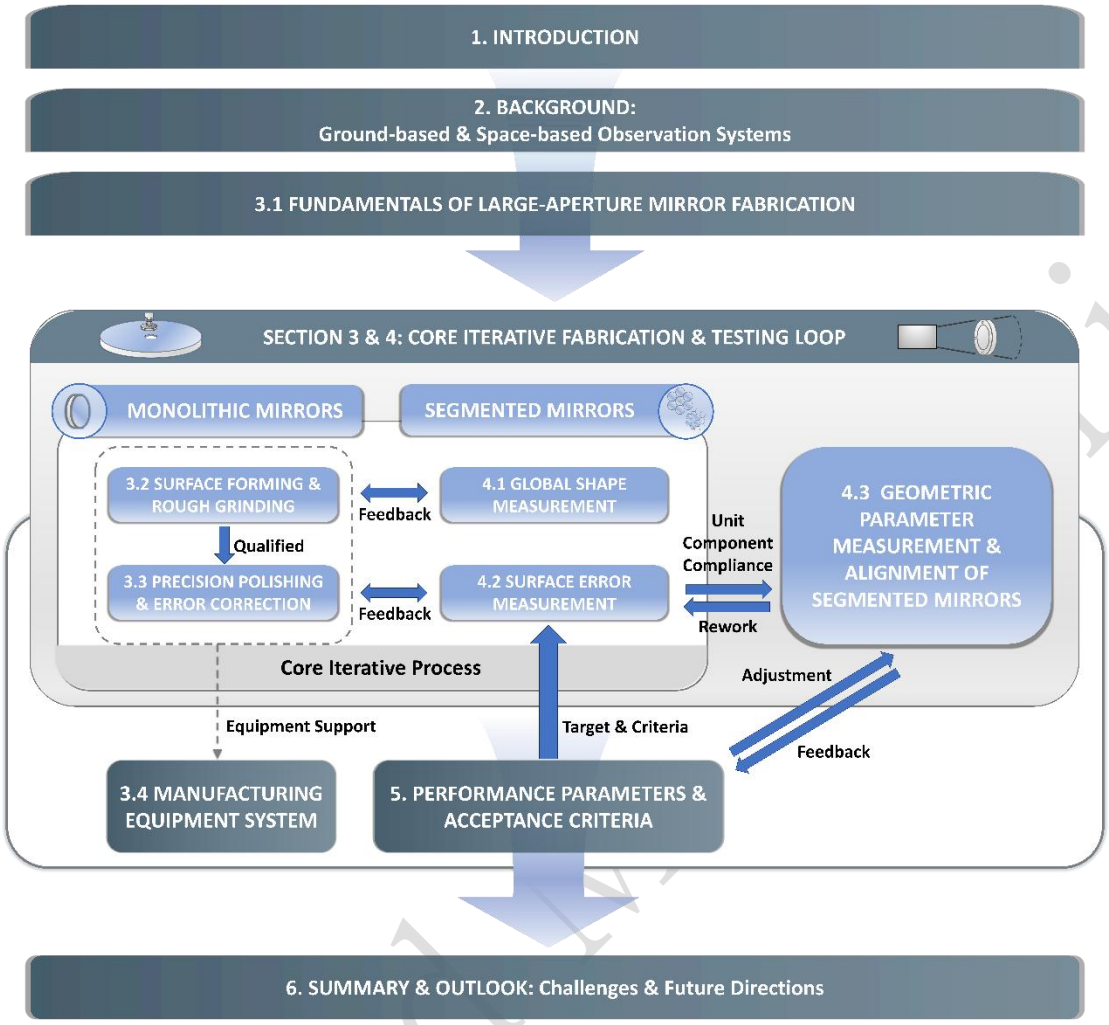

Fig. 1 Review frame

2. Application Background

Large-aperture optical mirrors are core components of modern astronomical telescopes. By increasing the collecting area and improving angular resolution, these mirrors enable telescopes to detect fainter objects, resolve finer spatial details, and acquire richer scientific data. Consequently, advances in large-aperture mirror fabrication and testing have become a key driving force behind the development of contemporary observational astronomy.

As outlined in the Introduction, this review summarizes representative manufacturing and testing methods for large-aperture optical mirrors used in major telescope systems worldwide. This section briefly introduces the scientific objectives, observational requirements, and operating wavelength ranges of representative

telescopes, while emphasizing the critical role of large-aperture mirrors in meeting these requirements.

According to their operating platforms and system roles, large-aperture telescope applications can be broadly divided into ground-based and space-based optical observation systems. In addition, several large-aperture mirrors have been developed as technology demonstrators or as non-mission-specific optical components; these mirrors are discussed separately because they provide important insight into advanced fabrication and metrology strategies.

2.1 Ground-based optical observation systems

Ground-based optical observation systems remain indispensable in astronomy. They provide crucial data for studying the origin and evolution of the universe, the formation and structure of galaxies, stellar evolution, exoplanets, and near-Earth objects. Their major advantages include large achievable aperture, maintainability, upgradeability, and compatibility with continuously evolving technologies such as adaptive optics, high-resolution spectroscopy, and wide-field imaging.

Representative examples include the 8.4 m NSF-DOE Vera C.[1, 2] Rubin Observatory, whose Legacy Survey of Space and Time are designed for wide-field optical and near-infrared time-domain surveys, including studies of dark matter, dark energy, transient phenomena, and small Solar System bodies; and the Gemini Observatory, which consists of twin 8.1 m optical/infrared telescopes used for multi-wavelength studies of star formation, galaxy evolution, supernovae, and exoplanets. These ground-based facilities complement space-based observatories and together form a coordinated, multi-wavelength observational framework. Additional representative ground-based telescope systems are summarized in Table 1.[3-15]

Table 1 Scientific objectives of typical ground-based telescope systems.

System name (abbreviation)	Maximum aperture (m)	Scientific objectives	Application wavelengths
Gran Telescopio Canarias (GTC)[10]	10.4	Analyzing the spectral information of stars, galaxies, black holes, the interstellar medium, etc.	Visible light, near-infrared, mid-infrared
Hobby–Eberly Telescope (HET)[5]	9.2	Exoplanet detection, galaxy research, and supernova studies	Visible light, near-infrared
W. M. Keck Observatory (Keck)[4]	10	Investigating the origin of stars and galaxies	Visible light, infrared
Bolshoi Teleskop Azimutalnyi (BTA; Large Altazimuth Telescope)[15]	6	Monitoring unknown celestial bodies; analyzing stellar temperature and composition	Visible light, infrared
Subaru Telescope (Subaru)[8]	8.2	Studying galaxy formation and exploring other habitable planets	Visible light, infrared
Very Large Telescope (VLT)[6]	8.2	Searching for nearby stars and studying stellar birth within nebulae	Visible light, near-infrared, mid-infrared
Giant Magellan Telescope (GMT)[12]	21.4	Searching for habitable planets; black hole and neutron star research; galaxy evolution	Visible light, near-infrared
Southern African Large Telescope (SALT)[7]	11	Quasar research; studying stars and galaxies	Visible light
Chinese Giant Solar Telescope (CGST)[16]	8	Precision measurement of the solar atmosphere's magnetic field and flow structures	Visible light, infrared
Southern Astrophysical Research Telescope (SOAR)[9]	4.1	Studying stars and galaxies	Visible light, near-infrared
Daniel K. Inouye Solar Telescope (DKIST)[17]	4	Solar magnetic field prediction	Visible light, near-infrared
Large Binocular Telescope (LBT)[11]	8.4	Studying stars and galaxies	Visible light, near-infrared
Extremely Large Telescope (ELT)[18]	39.3	Addressing fundamental issues in astrophysics	Visible light, near-infrared

Aperture values should be checked against the final citation set because different facilities report physical diameter, effective aperture, equivalent collecting aperture, or interferometric baseline in different ways.

Overall, ground-based large-aperture telescopes have continuously pushed the limits of optical fabrication, testing, alignment, and active control. They have greatly expanded the depth and breadth of astronomical observation. However, their performance is affected by atmospheric turbulence, absorption, scattering, thermal background radiation, and weather conditions. To access wavelength bands that are attenuated or blocked by the atmosphere and to achieve stable high-contrast

observations, space-based telescope platforms provide an essential complement to ground-based systems. This requirement has driven the development of a new generation of space-based optical observatories.

2.2 Space-based optical observation systems

Space-based optical observation systems operate above the Earth's atmosphere and therefore avoid atmospheric turbulence, absorption, scattering, and terrestrial background contamination. These advantages enable stable high-resolution and high-sensitivity observations, particularly in wavelength bands that are difficult or impossible to observe from the ground. Space telescopes are therefore essential for studying the early universe, galaxy evolution, stellar life cycles, exoplanet atmospheres, and faint or cold astronomical objects.

The development of space telescopes illustrates the increasing demand for larger apertures and higher optical performance. The Hubble Space Telescope, equipped with a 2.4 m primary mirror, greatly improved high-resolution imaging in the ultraviolet, visible, and near-infrared bands. The Herschel Space Observatory[19], with a 3.5 m silicon carbide primary mirror, extended astronomical observations into the far-infrared and submillimeter regimes and enabled studies of cold dust, molecular clouds, and early stages of star formation. The James Webb Space Telescope[20], featuring a 6.5 m segmented primary mirror, further advanced infrared astronomy and has opened new opportunities for investigating galaxy formation, exoplanets, and extreme cosmic environments.

The performance of flagship missions such as the James Webb Space Telescope represents a major achievement in optical engineering. Nevertheless, future scientific goals—such as observing fainter exoplanets, resolving more distant galaxies, and probing earlier stages of cosmic evolution—will require further improvements in aperture, wavefront control, thermal stability, deployment accuracy, and system-level optical performance. These requirements place increasingly stringent demands on optical fabrication and testing technologies, especially for lightweight, segmented,

and deployable large-aperture mirrors.

2.3 Exploration of new optical manufacturing and testing technologies

In addition to mirrors developed for specific telescope systems, several large-aperture mirrors have been fabricated as technology demonstrators or as representative components for future optical systems. Although they may not be directly associated with a single finalized telescope platform, their development addresses key technical challenges and provides valuable experience for advanced manufacturing and metrology. The diverse landscape of these next-generation systems and the key component technologies they drive are visualized in Fig. 2, which provides a framework for understanding the progression from system concepts to enabling manufacturing and metrology demonstrators.

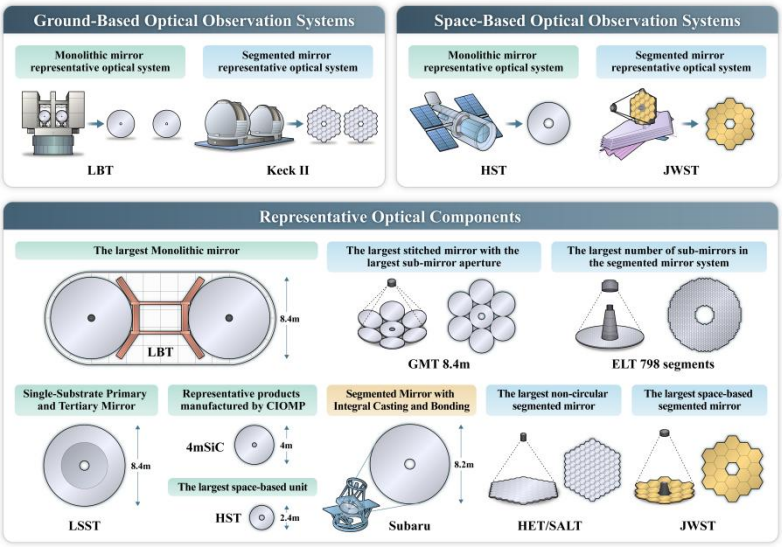

Fig. 2 Application Prospects of Emerging Manufacturing and Testing Technologies in the Field of Large-Aperture Optics

One representative example is the 4.03 m silicon carbide (SiC) aspheric mirror developed by the Changchun Institute of Optics, Fine Mechanics and Physics (CIOMP), Chinese Academy of Sciences.[21] This mirror represents a significant achievement in large-scale SiC mirror fabrication. Its lightweight mirror blank was produced using gel-casting and reaction-bonding-related technologies, while subsequent surface processing involved a combination of computer-controlled optical surfacing, stress-lap polishing, and magnetorheological finishing.[22, 23] For

high-precision surface measurement, methods such as computer-generated hologram null testing, swing-arm profilometry, phase deflectometry, and multi-source data fusion were employed to improve full-aperture surface figure measurement accuracy.[24]

The development of such mirrors demonstrates the importance of integrating mirror blank preparation, lightweight structural design, deterministic polishing, high-dynamic-range metrology, and error-separation algorithms. These efforts provide an important technical foundation for future large-scale SiC mirrors and for next-generation large-aperture optical systems. The specific manufacturing and testing methods involved in these developments are discussed in detail in the following sections.

3. Manufacturing of Large-Aperture Optical Mirrors

Manufacturing technologies for large-aperture optical mirrors are enabling foundations for modern astronomical observation, space exploration, and high-end precision optical systems. The fabrication of such mirrors is not a single process, but an integrated engineering chain involving mirror blank fabrication, structural design, surface generation, rough grinding, deterministic figuring, mechanical fixture support, and metrology feedback.

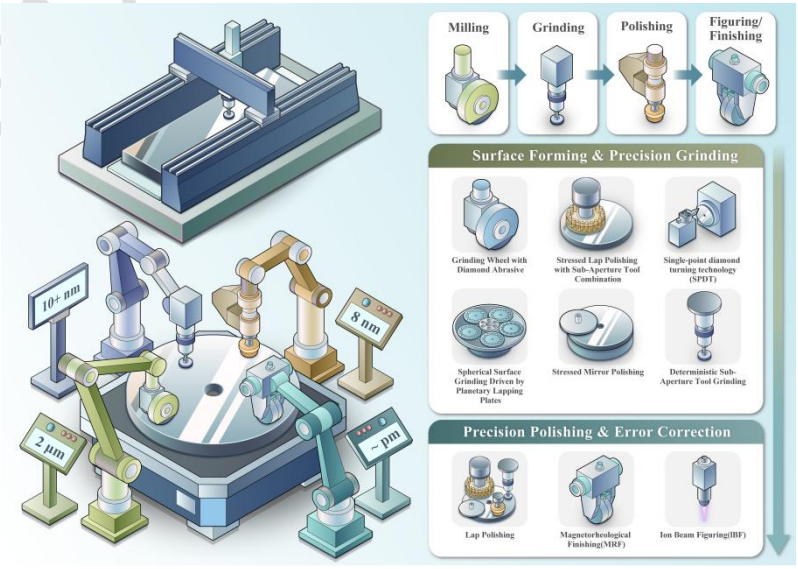

Fig. 3 Schematic overview of the integrated engineering chain for large-aperture optical mirror fabrication.

This section reviews the manufacturing routes of large-aperture optical mirrors from three perspectives. First, the basic mirror configurations, process routes, and key performance indicators are summarized. Second, the surface generation and rough grinding methods for monolithic and segmented mirrors are compared, with emphasis on fixed-abrasive and loose-abrasive processes. Third, precision polishing, and representative equipment systems are discussed. The purpose is to clarify how different technologies are selected and combined according to mirror material, aperture, surface form, spatial-frequency error, and system-level requirements.

3.1 Fundamentals of large-aperture mirror fabrication

Large-aperture optical mirror fabrication must balance optical performance, structural stability, manufacturability, and testing feasibility. Before discussing individual processes, it is necessary to clarify the main mirror architectures, typical manufacturing routes, and key indicators used to evaluate surface quality and system performance.

3.1.1 Main form of the primary mirror of the optical system

Large-aperture primary mirrors can be broadly classified into monolithic mirrors, segmented mirrors, and integrated multi-surface monolithic systems. Each configuration has distinct advantages and manufacturing challenges.

Monolithic mirrors provide a continuous optical surface and avoid segment phasing errors. However, the maximum aperture is constrained by blank fabrication, transportation, support deformation, thermal control, and full-aperture testing capability. Segmented mirrors overcome the aperture limit by combining multiple smaller elements, but they introduce additional requirements for segment-to-segment consistency, edge-effect control, active support, co-phasing, and system-level alignment. Integrated multi-surface monolithic systems, such as combined primary-tertiary mirrors, reduce alignment degrees of freedom by fabricating multiple

optical surfaces on one substrate, but they require extremely demanding synchronous generation, polishing, and testing strategies. In summary, the choice of system is a trade-off between the fabrication limits of monolithic substrates, the phasing and control complexity of segmented designs, and the advanced manufacturing required for integrated multi-surface mirrors. The fundamental distinctions and trade-offs among these three architectures are visually summarized in Fig. 4.

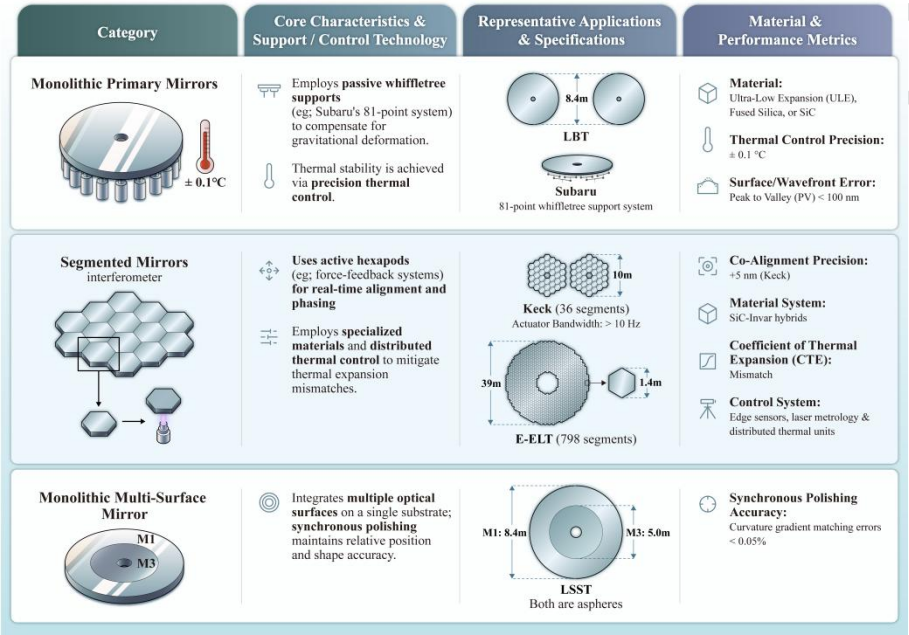

Fig. 4 Schematic comparison of three primary mirror architectures for large-aperture telescopes. The diagram contrasts the core concepts, support/control technologies, representative applications, and key specifications of (a) monolithic,[8, 25] (b) segmented,[26, 27] and (c) multi-surface monolithic mirror systems.[28]

3.1.2 Manufacturing process variations

Although process details vary with mirror material, aperture, and surface prescription, the general route for large-aperture mirror fabrication follows a staged convergence strategy. Bulk material is first removed to obtain the approximate geometry; rough grinding then reduces form error and establishes a controlled residual stock; precision polishing subsequently converge the surface figure from micrometer-level errors to nanometer-level accuracy. Throughout the process, metrology feedback is essential for dwell-time calculation, error separation, and process correction.

For monolithic mirrors, the main objective is to obtain a continuous high-quality surface while controlling low-frequency figure error, mid-spatial-frequency error, roughness, and support-induced deformation. For segmented mirrors, the objective extends beyond the quality of each individual segment. The manufacturing chain must also ensure segment-to-segment consistency, controlled edge gradients, compatible mechanical interfaces, and sufficient margin for active alignment and co-phasing. The key distinctions between the manufacturing processes for monolithic and segmented mirrors are contrasted visually in Fig. 5, moving from a tabular to a schematic representation for enhanced clarity.

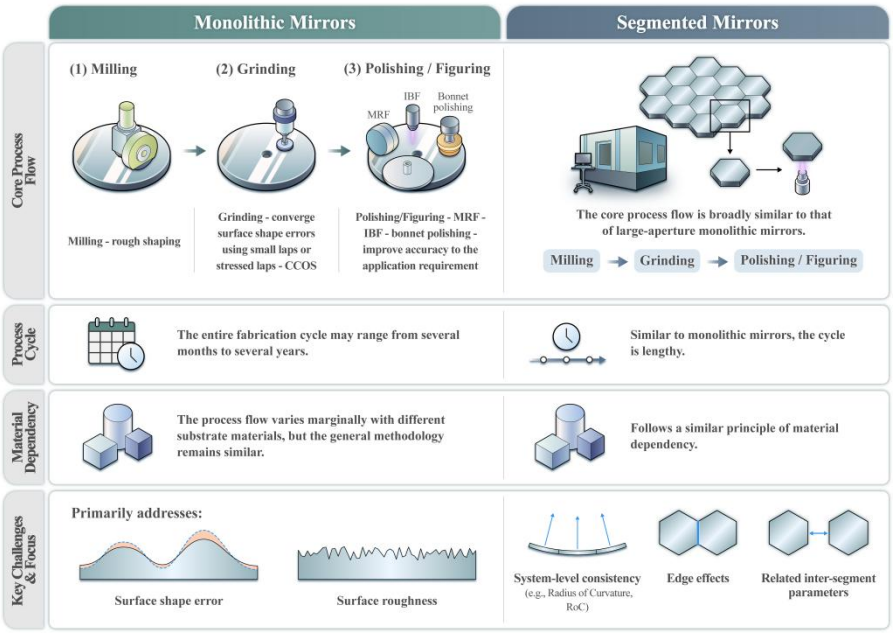

Fig. 5 Comparison of monolithic and segmented large-aperture mirror manufacturing processes.[21, 27, 29-37]

In contrast, the fabrication of segmented mirrors introduces an additional, critical layer of complexity: achieving system-level consistency. Beyond the quality of individual segments, manufacturers must ensure uniformity in parameters like the radius of curvature across all segments and manage edge effects and inter-segment relationships. This makes the process not just about creating excellent individual optical pieces, but about engineering them to function as a perfectly coherent single unit.

3.1.3 Key indicators

The performance of large-aperture optical mirrors is evaluated using a set of surface, structural, and system-level indicators. Surface figure error is usually described by PV and RMS values, while mid-spatial-frequency errors are commonly evaluated using PSD or band-limited RMS metrics. Surface roughness describes microscopic irregularities and is particularly important for controlling scatter, especially at short operating wavelengths. Subsurface damage is a hidden but critical factor introduced during grinding and must be removed or controlled before final polishing.

For segmented mirrors, additional indicators are required, including radius-of-curvature consistency, edge roll-off, segment clocking and indexing errors, actuator-interface accuracy, and residual co-phasing error. These indicators determine whether multiple segments can be assembled into an equivalent continuous aperture.

Table 2 Key Performance Indicators for Large-Aperture Reflecting Mirrors

Core Indicator	Description & Metrics	Practical Data & Examples
Surface Shape Accuracy	Represents the overall deviation of the optical surface from the ideal shape.[4, 38] Total Error: Measured by PV and RMS. Mid-frequency Errors: Controlled and evaluated using PSD[39, 40].	Keck Primary Mirror: PV < 80 nm;[4] E-ELT Sub-mirrors: RMS < 12 nm.[41]
Surface Roughness	Refers to microscopic irregularities on the surface[21, 40]	measured at the nm scale.
Other Considerations	Application-specific parameters that are critical for performance.	Subsurface Damage (SSD) Depth;[42] Radius of Curvature Matching (RoC);[20, 43] Segment Alignment & Phasing Parameters.[44, 45]

3.2 Surface forming and rough grinding

Surface generation and rough grinding form the foundation of the entire fabrication chain. At this stage, the main objectives are efficient material removal, reduction of gross figure error, control of residual stock, and suppression of subsurface damage. The selected process must match the substrate material, aperture, surface geometry, and expected spatial-frequency content of the residual error.

Two fundamental routes are commonly used: fixed-abrasive processing and

loose-abrasive processing. Fixed-abrasive methods, such as diamond grinding, use bonded abrasive grains and are well suited for deterministic shaping of hard and brittle materials such as SiC, ceramics, and some glass-ceramics. Loose-abrasive methods rely on free abrasives between the tool and workpiece, and they are widely used for large glass mirrors, spherical segments, and stressed-lap processes where conformal contact and smoothing are required.

Fixed abrasive grinding emphasizes deterministic control over hard, brittle materials and precision freeform surfaces. During the rough generation stage, the primary goal is efficient near-net-shape formation and control of subsurface damage within a removable allowance. For example, the Herschel 3.5 m SiC mirror blank after diamond grinding exhibited a surface form error on the order of ~100 μm relative to the best-fit paraboloid. The subsequent polishing and figuring stages were designed to converge the figure to ~1.5 μm RMS, roughness to <30 nm, and the final telescope wavefront error to <6 μm RMS. The grinding-induced SSD layer (typically a few μm) was deliberately kept within the stock removal budget of the later processes.[19]

In loose abrasive grinding, the use of specially designed tools such as stressed laps and flexible laps provides strong smoothing capability and conformal contact, making this approach particularly suitable for ultra-large-scale aspheric and freeform optics. Representative techniques include stressed-lap grinding, which dynamically matches the tool curvature to the local surface shape for efficient material removal and low-frequency error convergence (e.g., the 8.4 m primary-tertiary mirror of LSST[28]), and flexible-lap grinding, which uses passively deformable tools to accommodate steep off-axis geometries (e.g., the 4.2 m off-axis primary mirror of DKIST[46]). These methods are especially effective for mirrors with steep curvature gradients, such as the 1:5 steepness ratio of the LSST primary mirror,[47] where conformal contact and smoothing are critical for controlling mid-spatial-frequency errors.

Fig. 6 provides a systematic comparison of the two fundamental grinding methods. The primary distinction lies in the material removal mechanism. Loose abrasive grinding is characterized by a stochastic process where free abrasives remove material primarily through brittle fracture caused by indentation and rolling. In contrast, fixed abrasive grinding employs a deterministic, geometrically constrained process where bonded grains remove material via a combination of micro-cutting, scratching, and fracture. This difference in removal is governed by the underlying tool-abrasive contact mechanism. This fundamental difference stems from the fact that these methods exhibit distinct tool-abrasive contact mechanisms. The contact in loose abrasive processes is transient and random, with very short durations, while in fixed abrasive processes, it is sustained, periodic, and defined by the tool's geometry and path. These differing mechanisms directly result in their unique material responses and make each method suitable for specific applications and materials in large-aperture mirror fabrication.

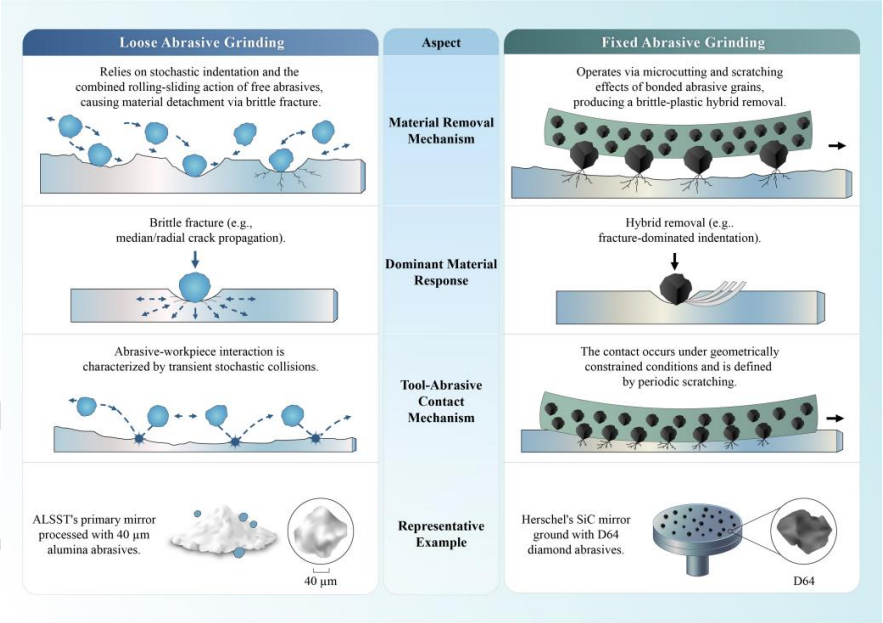

Fig. 6 Schematic comparison of loose abrasive grinding and fixed abrasive grinding mechanisms.[19, 28, 48-51]

3.2.1 Monolithic mirror fabrication

The surface forming and rough grinding of monolithic mirrors constitute a critical phase in achieving the desired optical prescription. This section details the

primary manufacturing methodologies, beginning with fixed abrasive milling for initial material removal and contour shaping. It then explores loose abrasive grinding, with a specific focus on advanced techniques like stressed-lap grinding that actively control the tool's shape to correct for errors and efficiently converge the surface figure. Finally, a summary will be provided to compare these approaches and outline their respective roles in the fabrication workflow.

3.2.1.1 Fixed abrasive milling/grinding

Fixed-abrasive generation is frequently used when the substrate is hard, brittle, or difficult to process using conventional loose-abrasive methods. Diamond grinding is the most representative process. Diamond abrasives embedded in a wheel or tool remove material through micro-cutting, frictional sliding, and ploughing. For brittle materials, the process may also induce median and lateral cracks; therefore, the control of grinding parameters is essential for limiting SSD and ensuring the efficiency and integrity of the subsequent manufacturing stages.

A representative example is the 3.5 m silicon carbide primary mirror of the Herschel Space Observatory.[52] Because SiC has high stiffness and thermal stability but also high hardness and brittleness, diamond grinding was adopted during rough generation. The process demonstrated high removal efficiency and controllable surface roughness, but also required careful management of edge-removal fluctuations, tool wear, and residual microcracks. These issues illustrate the central trade-off of fixed-abrasive grinding: it is efficient and deterministic, but must be integrated with subsequent fine grinding and polishing steps to remove or reduce SSD.[53, 54]

3.2.1.2 Loose abrasive grinding

Loose-abrasive grinding is widely used in large glass mirror fabrication because it provides strong smoothing capability and can be combined with large-area conformal tools. Among loose-abrasive methods, stressed-lap grinding is particularly important for large aspheric mirrors. A stressed lap is an actively deformable tool whose curvature is adjusted to match the local curvature of the workpiece. This

enables high material removal efficiency while maintaining conformal contact and suppressing mid-spatial-frequency errors.[55, 56]

The Multiple Mirror Telescope (MMT) established an important technical basis for subsequent large honeycomb mirrors.[57] Its fabrication used large CNC generation combined with stressed-lap processing to converge the surface from millimeter-scale casting error toward micrometer-level accuracy. The stressed lap also provided passive smoothing, reducing mid-to-high spatial-frequency errors during rough and intermediate stages.[58, 59]

The Rubin Observatory/LSST M1M3 mirror further illustrates the role of stressed-lap processing in complex monolithic systems. The combined primary-tertiary mirror requires coordinated shaping of two aspheric surfaces on a single substrate. Large stressed laps and smaller correction tools were used in combination to remove material efficiently while controlling the different curvature requirements of M1 and M3.[47, 60] Similarly, the off-axis primary mirror of DKIST used active and passive flexible laps to manage the combined challenges of off-axis geometry, large aperture, and high surface-quality requirements.[46, 61]

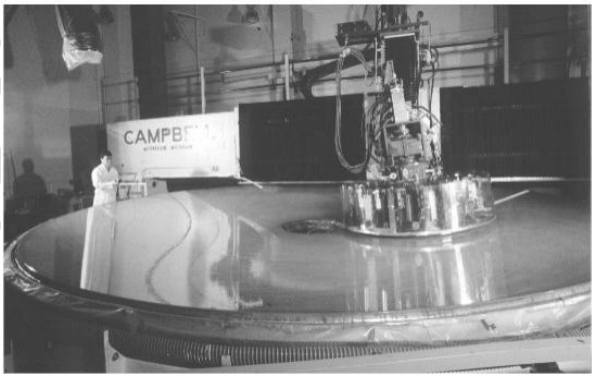

Fig. 7 Schematic of stressed-lap processing integrated with a large-scale CNC machine tool.[58]

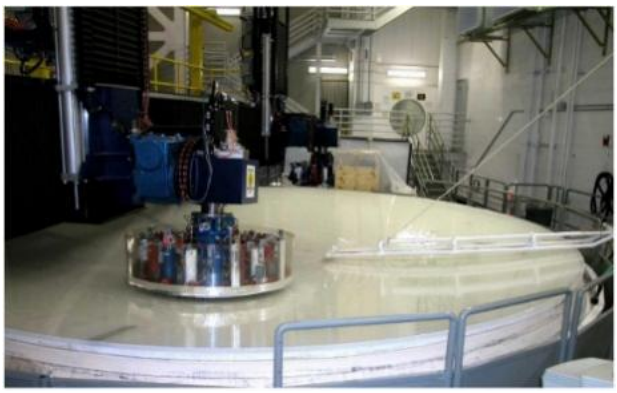

Fig. 8 Mirror Lab's 8.4 m capacity large grinding machine. The photo shows two 1.2 m stressed laps.[60]

3.2.1.3 Chapter Summary

For monolithic mirrors, rough generation must be selected according to material properties and surface geometry. Fixed-abrasive grinding provides efficient deterministic shaping for hard and brittle substrates, but requires strict SSD and tool-wear control. Loose-abrasive processes, particularly when combined with stressed-lap tools, are more suitable for large glass mirrors and steep aspheres because they provide conformal contact, smoothing, and efficient convergence of low- and mid-frequency errors. In practice, high-precision fabrication of large-aperture mirrors often combine these routes to balance material removal rate, damage control, and subsequent polishing efficiency.

Table 3 Summary of Rough Grinding Technologies for Large Optical Mirrors

Feature	Fixed Abrasive Milling (Diamond Grinding)	Loose Abrasive Grinding (Stressed-Lap)	Loose Abrasive Grinding (Flexible Lap)
Category	Fixed Abrasive Milling[62]	Loose Abrasive Grinding[63]	Loose Abrasive Grinding[64]
Technology	Diamond Grinding	Stressed-Lap Grinding[65]	FLEX Lap Grinding
Principle	Material removal via micro-cutting, frictional sliding, and ploughing using diamond-embedded grinding wheels.[66]	Achieves conformal contact using a controllably deformable lap, based on Hertzian contact theory and active optics.[67]	Material removal via random collisions and scratching by free abrasives using multi-size flexible laps.[68]
Key Characteristics	High material removal rate (MRR). Effective for hard/brittle materials. Brittle-fracture-dominated removal.	High adaptability to aspheric surfaces. High-efficiency material removal (>90%). Synchronous multi-scale error control.[69]	Precise material removal. Suitable for complex off-axis surfaces. Enables synergy between rough and fine grinding.
Applicable	Cemented carbides,	Optical glass substrates	Large off-axis aspheric

Materials	Ceramics, Optical glasses, Sapphire, Semiconductor wafers, Polycrystalline diamond.	(e.g., borosilicate, ULE). SiC mirrors >4m. Steep aspheres (ratio >1:10).	mirrors.
Representative Applications	Herschel Space Observatory: 3.5 m SiC primary mirror.[54]	LSST: 8.4 m primary-tertiary mirror.[60]	DKIST: 4.2 m off-axis primary mirror (coarse & fine grinding).[46]
Challenges & Notes	Fluctuating MRR at edges. Micro-crack formation. Significant grinding wheel wear. Requires balancing efficiency with SSD control.	Highly dependent on high-precision motion systems and real-time deformation control algorithms.	Requires computer-controlled multi-axis systems and optimized abrasive grit sizes.[56]

In conclusion, the selection of a rough grinding technology involves a fundamental trade-off between efficiency, precision, and damage control. No single technology is universally superior. The success of modern large-scale projects (such as Herschel, LSST, and DKIST) hinges on selecting or hybridizing the most appropriate rough grinding strategy based on specific material properties, surface form requirements, and production timelines. This strategic choice is crucial for ensuring that the process provides sufficient and predictable material allowance for the subsequent fine grinding and polishing stages to achieve the final nanometer-level accuracy.

3.2.2 Segmented mirror fabrication

Segmented mirror fabrication addresses the manufacturing of extremely large-aperture optical systems by combining multiple mirror segments. The process employs two primary technological pathways: fixed abrasive milling for efficient material removal and deterministic shaping of individual segments, and loose abrasive grinding, which encompasses several advanced methods. These include spherical surface grinding driven by planetary lapping plates for uniform stock removal, stressed-lap grinding for conformal aspheric shaping, stressed mirror polishing for precise figure correction by actively bending the mirror, and deterministic sub-aperture tool grinding for controlling mid-to-high spatial frequency errors. This suite of techniques ensures that each segment achieves the required surface figure and quality while meeting the critical co-phasing requirements for the final assembled

mirror.

3.2.2.1 Fixed abrasive milling/grinding

Segmented mirrors require not only accurate surface generation of each segment, but also strict control of thickness, edge geometry, support interfaces, and segment-to-segment consistency. Fixed-abrasive milling and diamond grinding are therefore used when deterministic shaping and high removal efficiency are required. For off-axis aspheric segments, such as those used in the GMT,[12] computer-controlled generation provides the initial off-axis geometry and reduces the burden on subsequent stressed-lap polishing and local figuring.

3.2.2.2 Loose abrasive grinding

For segmented mirrors with spherical or near-spherical prescriptions, planetary lapping and loose-abrasive grinding provide efficient and repeatable processing routes. HET,[70] SALT,[71] and LAMOST[72] illustrate this approach. By matching the curvature of the tool and segment surface, planetary grinding can provide stable material removal and good surface smoothing for large batches of spherical segments.

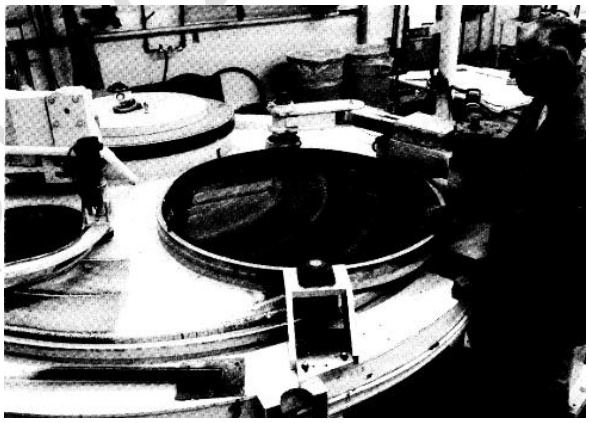

Fig. 9 Planetary polishing machine.[70]

For off-axis or strongly aspheric segments, more advanced strategies are required. Stressed-lap grinding uses a deformable tool to maintain conformal contact with each segment, while stressed-mirror polishing deforms the segment itself into a more easily polished shape. After unloading, elastic spring-back produces the target aspheric figure. This principle was used in the fabrication of Keck segments and has also been

studied for next-generation segmented telescopes.[4, 73] Deterministic sub-aperture grinding and small-lap correction complement large-tool methods. Large tools are efficient for low-frequency and global errors, whereas small tools can correct edge roll-off, mid-frequency waviness, and local residual errors. A hierarchical tool chain, combining large stressed laps, rigid conformal tools, and smaller correction tools, is therefore essential for segmented mirror fabrication.

3.2.2.3 Chapter Summary

Compared with monolithic mirrors, segmented mirror fabrication places stronger emphasis on batch consistency, edge control, and system-level compatibility. Each segment must meet individual surface specifications while also preserving geometric correlations with the full primary mirror. Effective rough-generation strategies therefore combine multi-scale tooling, elastic deformation models, process-specific SSD control, and metrology-guided error separation.

Table 4 Coarse Grinding of Segmented Mirrors

Category	Specific Challenge	Core Technical Approach	Representative Project	Key Technical Indicator
Major Challenges	Non-continuous surface shape convergence	Pre-deformation of segments to a machinable shape.	Keck Telescope: Pre-deformation stress disk technology using asymmetric force fields.[74]	Decomposed global asphere into locally spherical base (6.8 mm compensation).
Major Challenges	Edge collapse compensation	Dynamic adjustment of pressure distribution at edges.	GMT: Combined 1.5 m stressed lap with 40 cm passive grinding lap.[75]	Effectively suppressed edge collapse during rough grinding.
Major Challenges	Cross-scale error coupling	Isolating and correcting errors at different spatial frequencies.	HET: Planetary grinders (Φ2.5 m) combined with cylindrical grinders.[76]	Isolated full-aperture low-frequency from mid-frequency errors in splice region.
Sub-mirror Geometric Correlation Control	Aspheric Surface Decomposition	Pre-deformation via elastic mechanics modeling.	Keck Telescope[69]	Achieved locally machinable spherical surface.
Sub-mirror Geometric Correlation Control	Edge Effect Mitigation	Multi-size tooling for tailored pressure distribution.	GMT Project[77]	Controlled material removal rate at critical edges.
Dynamic Error Decoupling	Multi-scale Error Separation	Synergistic use of large and small tools in a toolchain.	HET Project: Planetary grinder + cylindrical grinder	Removed 90% material with loose abrasives; corrected

Strategy			+ small-lap process.[70]	residual high-frequency errors.
Dynamic Error Decoupling Strategy	Heterogeneous Material Processing	Corrected contact model for non-uniform substrates.	MMT Project: Hertzian contact model with equivalent elastic modulus correction (1.12-1.18).[78]	Reduced removal rate discrepancy from 15% to < 8%.
Surface Forming Accuracy Guarantee	Surface & Sub-surface Quality Control	Gradient abrasive process (multi-grit sizes).	SDSS Project: 40 μm Al2O3 + 9μm diamond composite abrasives[79].	Simultaneously achieved Ra < 0.5 μm and SSD < 18 μm.
Surface Forming Accuracy Guarantee	In-situ Metrology & Correction	Dynamic path correction based on regular error mapping.[72]	LAMOST System: Laser tracker + contact profilometer feedback.	Converged gradient error in spliced area to 0.3 μm/mm.
Conclusion	Integrated Solution	Combines multi-tool strategies,[70] cross-scale error decoupling,[76] and material-specific optimization.[78]	General Approach	Ensures uniform subsurface integrity and controlled residual stock for polishing.

In conclusion, the grinding of segmented mirrors necessitates integrated solutions that combine multi-tool strategies (e.g., stressed laps for global errors and sub-aperture tools for mid-to-high frequency correction), cross-scale error decoupling, and material-specific process optimization. These approaches ensure uniform subsurface integrity and controlled residual stock for the subsequent polishing stage.

3.3 Precision polishing and error correction

Precision polishing convert the surface produced by grinding into an optical-quality mirror. Modern large-aperture polishing is usually based on computer-controlled optical surfacing. The removal distribution is calculated from measured surface error, a calibrated removal function, and a dwell-time algorithm. The process is therefore deterministic, metrology-driven, and iterative.

Different technologies operate most effectively over different spatial-frequency ranges. Large stressed laps and compliant tools are efficient for low-frequency and large-scale errors; small tools and MRF are effective for mid-spatial-frequency and local errors; IBF provides non-contact final figuring and is especially useful when residual error must be corrected without introducing mechanical stress.

3.3.1 Monolithic mirror fabrication

The manufacture of monolithic large-diameter optical elements presents significant challenges, including extremely high demands on process stability, high scrap rates, prolonged grinding and polishing durations, difficulties in managing gravity-induced deformation and mechanical support, and limitations in full-aperture testing equipment. In response to these challenges, numerous advanced polishing technologies have been developed, as detailed in the following subsections.

3.3.1.1 Stressed-lap polishing (SLP) with sub-aperture tool combination

Stressed-lap polishing (SLP) is a key technology for large aspheric monolithic mirrors. By actively adjusting the shape of a deformable lap, SLP maintains near-conformal contact with the mirror surface. This enables relatively high removal rates while providing smoothing and low-frequency figure convergence.

In practice, SLP is often used in combination with smaller sub-aperture tools. The large stressed lap removes broad, low-frequency errors and maintains global smoothness, while small tools correct localized residual errors, edge zones, and mid-spatial-frequency features. This multi-tool strategy has been applied in the fabrication of large telescope mirrors such as LSST/Rubin M1M3,[47, 60, 80] SOAR,[8, 9, 81] LBT,[11, 25, 58, 82] Subaru,[8, 9] and other 8 m-class systems.

The main advantages of SLP are high material removal efficiency, curvature adaptability, and effective control of large-scale figure errors. Its limitations include actuator bandwidth, calibration of lap deformation, wear of polishing layers, thermal-mechanical coupling, and the need for accurate dwell-time planning.

Fig. 10 Two views of the combined LSST M1 and M3 being polished. Left: 1.2 m stressed lap on M3 and 25 cm orbital lap on M1, with zirconium oxide polishing compound. Right: stressed lap polishing M1 with rouge (iron oxide).[80]

Fig. 11 Primary mirror being optically fabricated using Goodrich's large computer-controlled grinding and polishing machine.[9]

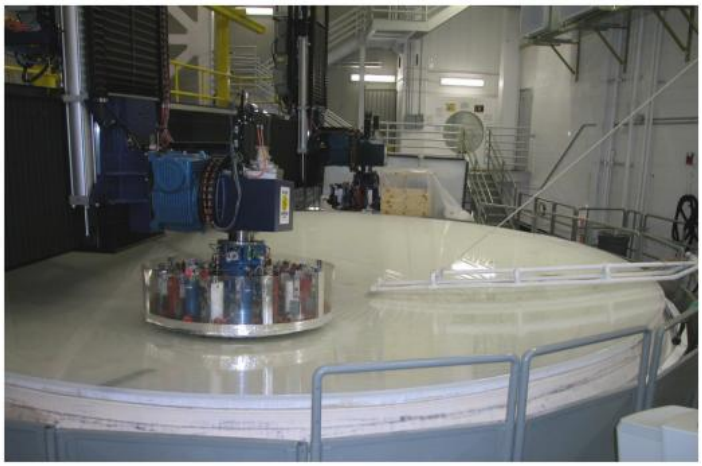

Fig. 12 Stressed-lap polishing of the second LBT mirror on the new 8.4 m polisher.[82]

Table 5 Advantages and Challenges of Stressed-Lap Polishing Technology

Advantages	Challenges
Dynamic curvature matching enables	Limited response bandwidth of large actuators

high-precision surface shape control.[11, 82]	restricts dynamic adjustment speed.
Rigid-flexible composite tool design achieves material removal rates >10 μm/h.[60]	Complex asphalt/ceramic layer wear requires calibration and maintenance every 48 hours.[80]
Multi-tool collaborative control supports error separation efficiency >80%.[47]	Modeling thermo-mechanical coupling in steep asphere processing is challenging, affecting stability.[58]

Together, these advantages and challenges define the current state of stressed-lap polishing technology in large-aperture optical fabrication.

3.3.1.2 Magnetorheological Finishing (MRF)

Magnetorheological finishing uses a magnetically stiffened polishing fluid to form a controllable, flexible removal zone. Under a magnetic field, the magnetorheological fluid develops a localized yield stress and behaves like a compliant polishing tool. The removal function is typically stable and deterministic, making MRF effective for correcting mid- and high-spatial-frequency errors.[83-87]

MRF has been applied to a wide range of optical components, including off-axis aspheres and large SiC mirrors. Reported cases include 1.5 m-class off-axis aspheric mirrors,[84, 88, 89] 2 m SiC mirrors,[89, 90] and the 4.03 m SiC mirror developed by CIOMP[23, 91]. These demonstrations show that MRF can significantly improve figure accuracy and reduce residual errors after conventional polishing.

The main strengths of MRF are deterministic convergence, low mechanical loading, good local correction capability, and suitability for complex aspheres. Its main limitations are relatively low removal efficiency for very large apertures, sensitivity to removal-function stability, slurry management, and the need to integrate MRF with upstream smoothing and downstream final testing.

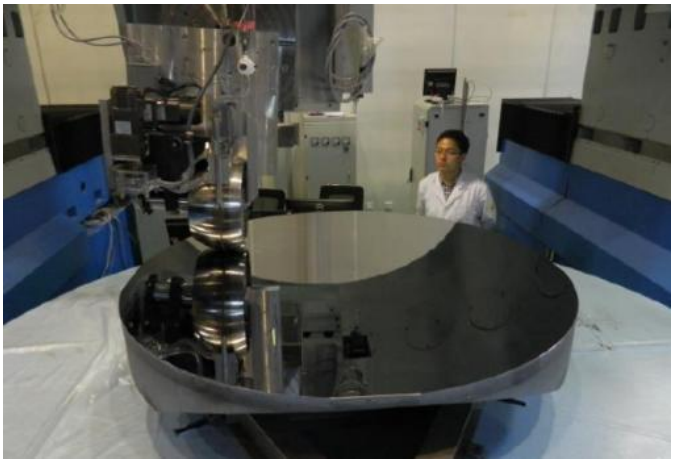

Fig. 13 MRF process.[84]

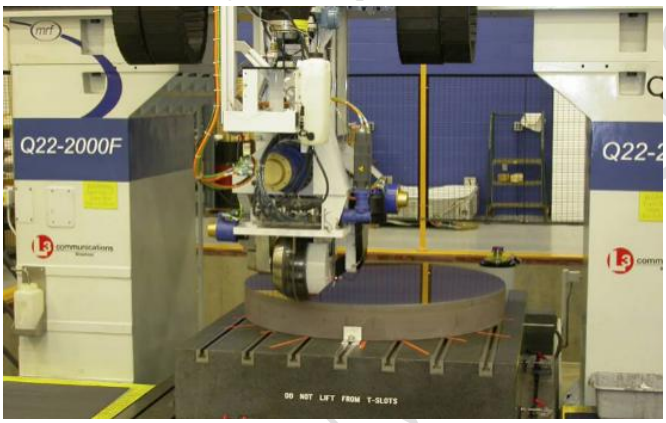

Fig. 14 Q22-2000F MRF polishing machine, commissioned in July 2008, used for 1.5 m diameter optics.

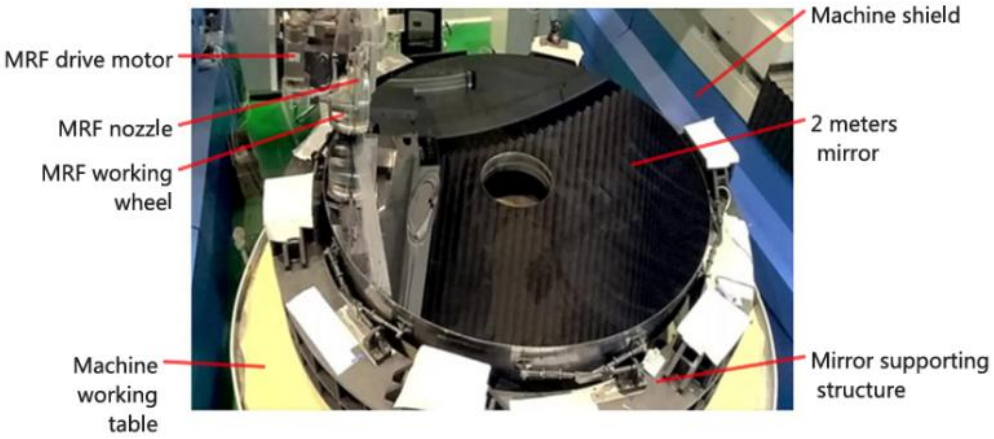

Fig. 15 2 m SiC mirror after polishing.[90]

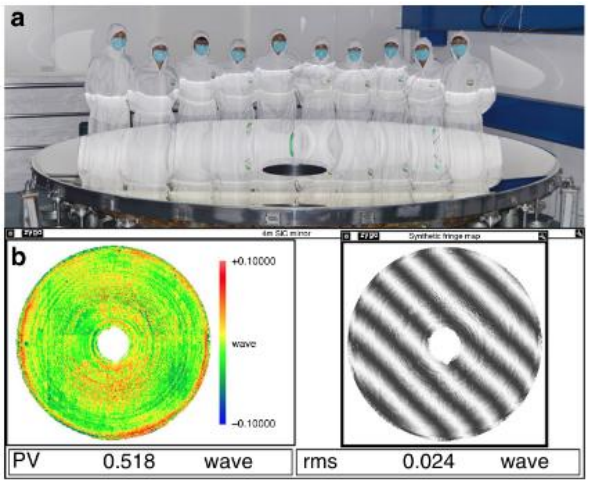

Fig. 16 (a) Photograph of the world's largest ⌀4.03 m SiC aspheric mirror. (b) Test result and interferogram of the ⌀4 m SiC mirror.[21]

MRF establishes itself as a pivotal technology in modern optics manufacturing. Its capacity for deterministic error correction and subsurface damage elimination enables the production of high-precision surfaces with rapid convergence. However, the technology's full potential in production environments remains contingent upon overcoming key challenges, particularly in enhancing removal efficiency, improving process repeatability, and scaling for broader industrial implementation.

The MRF technology is experiencing rapid development. In recent years, its processing strategies,[92] equipment,[93] mechanisms,[94, 95] processes,[96, 97] prediction models,[98, 99] paths,[100] etc. have been extensively studied.

3.3.1.3 Ion Beam Figuring (IBF)

Ion beam figuring is a non-contact deterministic figuring process based on atomic-scale sputtering. Inert gas ions are accelerated and directed toward the optical surface, removing material through momentum transfer. Because the process is contactless, IBF does not introduce mechanical stress, tool marks, or additional subsurface damage. It is therefore often used as a final figuring step after mechanical polishing.[44, 45, 101]

IBF is particularly suitable for correcting residual figure errors on high-precision aspheric surfaces and segmented mirrors. For example, it has been used in the final correction of large telescope components such as the LSST/Rubin secondary mirror

and mirror segments for segmented telescopes. Its main challenges are relatively low material removal rate, high equipment cost, the need for a vacuum chamber, and possible thermal effects induced by localized beam energy.[102]

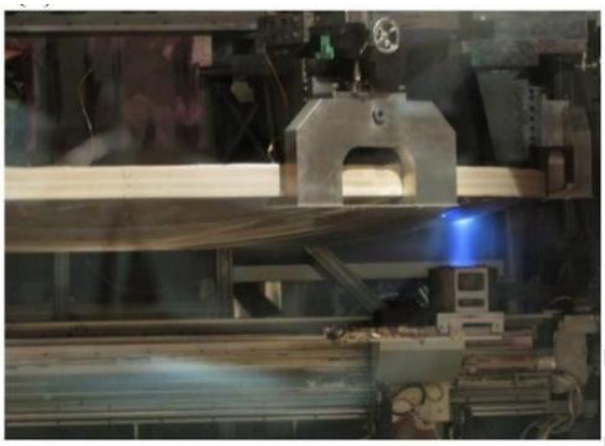

Fig. 17 Device developed by Harris Corporation.[102]

3.3.1.4 Chapter Summary

For monolithic mirrors, SLP, MRF, and IBF form a complementary process chain. SLP provides efficient large-scale convergence; MRF corrects local and mid-spatial-frequency residuals with high determinism; and IBF provides non-contact final correction at nanometer or sub-nanometer scale. The optimal process route is usually hybrid rather than single-technology based.

3.3.2 Segmented mirror fabrication

When polishing segmented mirrors, the manufacturing objective shifts from producing a single continuous surface to producing many mutually consistent segments. Each segment must meet its own surface figure and roughness specifications, but it must also satisfy system-level requirements for edge quality, radius of curvature, actuator interfaces, and co-phasing.

Small-lap CCOS is widely used for segment polishing because segment dimensions are smaller than monolithic mirrors and local correction is often efficient. For LAMOST segments, [72, 103] deterministic small-tool polishing combined with interferometric feedback enabled high-accuracy spherical segment fabrication. For

Keck, [4, 73, 74, 104] GMT,[105, 106] and other segmented systems, small tools complement stressed-lap or stressed-mirror processes by correcting residual local errors and edge zones.

3.3.2.1 Stressed-lap, stressed-mirror, and small-lap polishing

Stressed-lap polishing remains important for large off-axis or aspheric segments because it provides efficient low-frequency convergence. Stressed-mirror polishing provides another route: the segment is elastically deformed into a more easily polished shape and then released to obtain the target aspheric surface. This strategy can be efficient for thin or flexible segments, but it requires accurate elastic modeling, precise loading, and careful edge compensation.

Fig. 18 Optical component preliminary polishing.[72]

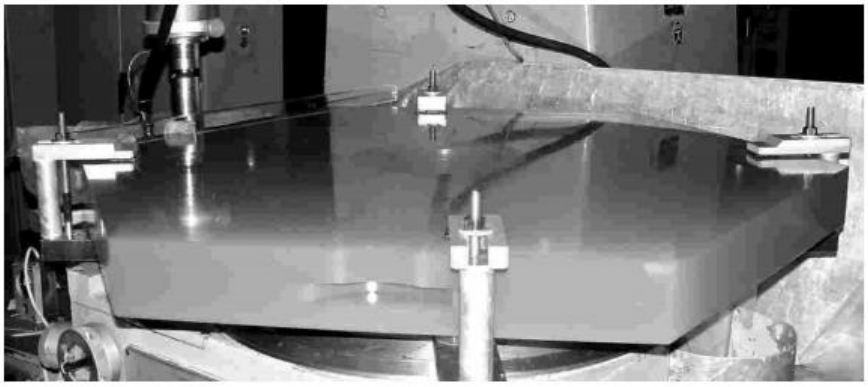

Fig. 19 LAMOST sub-mirror milling.[72]

Small-lap polishing and deterministic CCOS are essential for final correction of segment-level residuals. By combining tool-size selection, dwell-time optimization,

and boundary-control strategies, small tools can suppress mid-frequency error, edge roll-off, and local ripple. The resulting process chain is usually hierarchical: large tools handle global figure, intermediate tools handle regional errors, and small tools handle local residuals.

3.3.2.2 IBF for segmented mirrors

IBF is particularly valuable for segmented mirrors because it can correct residual errors near edges without mechanical contact. The process has been reported in the fabrication or final figuring of segments for telescopes such as GTC[107, 108], Keck-related segment development,[4, 26, 73, 74] ELT,[14, 35, 109-111] and other large segmented systems. Its ability to perform non-contact local correction makes it suitable for high-accuracy edge zones and final figure correction.

Fig. 20 GTC primary mirror undergoing ion beam shaping.[108]

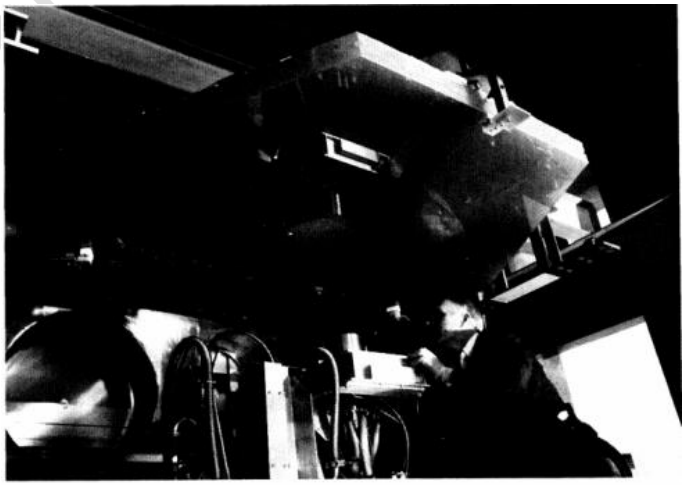

Fig. 21 Keck PM segment supported in a 2.5 m ion figuring system using a three-pad

support fixture.[4]

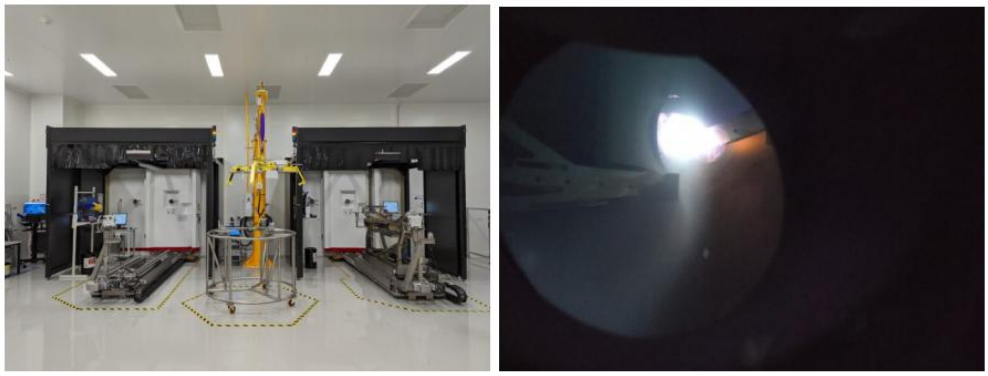

Fig. 22 (a) Two IBF machines. (b) Ion beam on the segment surface inside the vacuum chamber.[86]

The main engineering constraints of IBF are chamber size, throughput, thermal management, and cost. For mass production of hundreds of mirror segments, these constraints require careful process scheduling, standardized fixtures, stable removal-function calibration, and efficient metrology feedback.

3.3.2.3 Single-point diamond turning (SPDT)

Single-point diamond turning is an ultra-precision machining technology especially suitable for metallic mirrors and selected infrared optical components. It can generate optical surfaces with high geometric accuracy and low roughness on materials such as aluminum alloys and some beryllium-based substrates. In space optics, SPDT is attractive because it can combine lightweight metal substrates with deterministic machining.

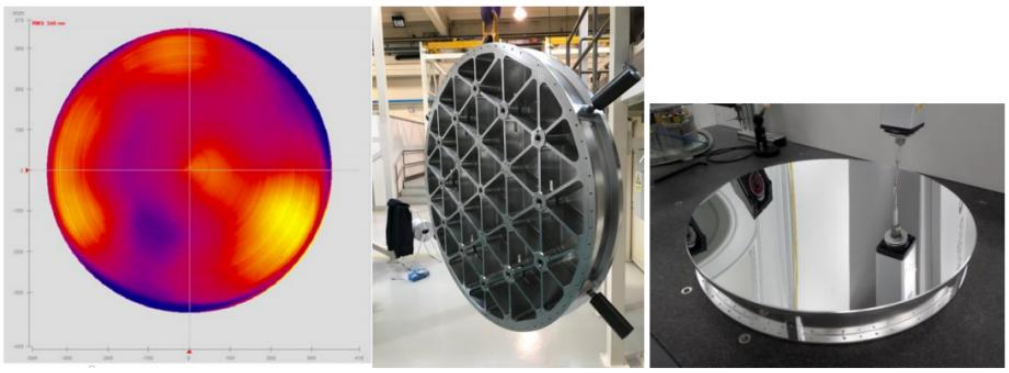

Fig. 23 Prototype mirror after diamond turning.[112, 113]

It should be noted that SPDT is fundamentally different from conventional

optical polishing methods. It is not a routine surface smoothing technique, but rather a precision machining process. Therefore, SPDT is typically reserved for specific applications requiring the fabrication of specialized infrared optical components or those made of special materials, rather than for the final figuring of general large-aperture reflective mirrors.

The Ariel telescope mirror development provides a representative example of aluminum mirror fabrication using SPDT. Prototype mirrors demonstrated that diamond turning can achieve sub-micrometer figure accuracy and nanometer-level roughness on aluminum substrates. Nevertheless, tool wear, cutting-force variation, material anisotropy, and residual turning marks remain important challenges for large mirrors and batch production. For beryllium mirrors, SPDT is relevant as a manufacturing possibility, but any project-specific claim should be supported by primary manufacturing documentation.[112-116]

3.3.2.4 Chapter Summary

For segmented mirrors, polishing and figuring technologies must support both optical precision and system integration. Stressed-lap and stressed-mirror processes provide efficient low-frequency correction; small-lap CCOS offers flexible local correction; MRF provides deterministic mid-frequency error control; IBF enables non-contact final figuring; and SPDT is useful for selected metal-mirror applications. Future development will focus on production repeatability, edge control, automated metrology feedback, and cross-scale error management for hundreds of segments.

3.4 Manufacturing equipment system comprehensive survey

Large-aperture optical fabrication depends on specialized equipment systems. These systems must provide not only sufficient mechanical range and stiffness, but also high thermal stability, controllable tool pressure, precise trajectory execution, and compatibility with in-process or off-line metrology. Equipment development has therefore become a central part of large mirror manufacturing capability.

The major equipment categories include ultra-precision CNC generation machines, large polishing machines, deterministic figuring systems, robotic polishing systems, and large-scale testing-compatible support platforms. These systems are increasingly integrated with digital process planning and closed-loop metrology.

3.4.1 Ultra-precision CNC machines

Ultra-precision CNC machines and large optical generators are used for initial surface generation, backside machining, lightweight mechanical fixture support preparation, and deterministic grinding. Their performance depends on multi-axis motion accuracy, dynamic stiffness, thermal stability, tool-path planning, and error compensation. In large mirror fabrication, absolute positioning accuracy is important, but stable and repeatable dwell-time or tool-path execution is often more critical for deterministic material removal.

For off-axis or freeform segments, CNC machines must control tool orientation, contact pressure, and local removal while avoiding edge damage and excessive SSD. Future development will continue to emphasize machine thermal control, dynamic-error compensation, and integration with measured surface maps.

In practice, many dedicated polishing systems are built upon ultra-precision CNC platforms. Dedicated polishing equipment is designed for specific process requirements in large-aperture mirror fabrication. Examples include large polishing machines with dual heads, stressed-lap systems, large optical generators, and large IBF chambers. These systems are often developed in close connection with particular telescope projects and then become enabling platforms for subsequent mirrors.

As shown in the table below. The University of Arizona large polishing machines demonstrate the value of multi-tool coordination, combining large stressed laps for rapid convergence with smaller tools for local correction. Large optical generators provide the deterministic shaping capability needed for large off-axis segments such as those used in GMT. Large-scale IBF systems provide non-contact final figuring for high-precision segmented mirrors, although chamber size and throughput remain

major constraints.

Table 6 Dedicated polishing equipment processing project information form.

Manufacturing unit	Dedicated polishing equipment	Processing project	Specific circumstances
University of Arizona	Large optical generator	LBT	Secondary main mirror (8.4 m); used for fine grinding to final dimensions.
		LSST	Main mirror (8.4 m); part of the dual-head LPM, supporting stressed disk and sub-aperture tool operation.
		GMT	Off-axis lens section (8.4 m); completed surface generation and fine grinding of segments S2, S3, and S5.
SAGEM-REOSC	IBF	GTC	Primary mirror (10.4 m, composite); final surface correction of 36 hexagonal sub-mirrors.
		GTC	Secondary mirror (M2, 1.18 m); final shaping after high-precision aspheric polishing.
University of Arizona	Dual-head LPM	LSST	Simultaneous processing of concentric main mirror (RC rigid disk) and tertiary mirror (1.2 m stressed lap).
		GMT	Off-axis segment (8.4 m); dual-tool coordinated shaping (e.g., 1.2 m stressed lap + 27 cm RC flexible disk) for tertiary mirror segment.
		LBT	Basic equipment prototype supporting dual stressed laps or stressed lap/local shaping tool combinations.

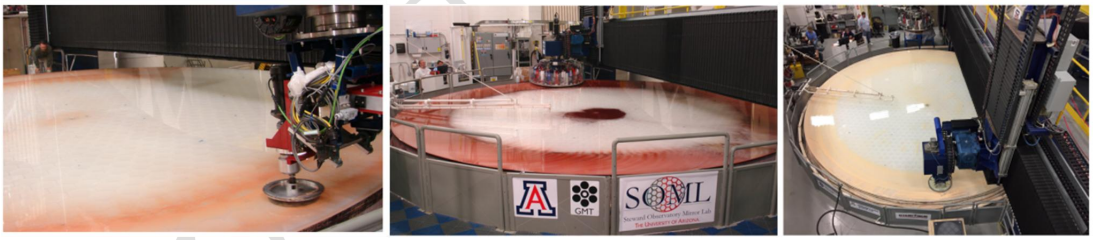

Fig. 24 Dual-head LPM.[75]

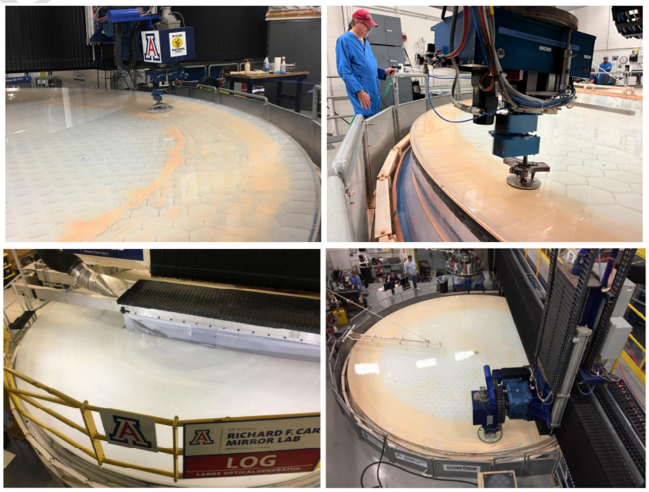

Fig. 25 8.4 m CNC large-scale optical grinding machine (large optical generator).[77, 117, 118]

Fig. 26 2.5 m large IBF chamber.[107, 108]

3.4.2 Robotic polishing systems

Robotic polishing systems provide flexible multi-degree-of-freedom motion and are well suited for complex surfaces, large lightweight mirrors, and components that require adaptive tool orientation. A robotic platform can combine force-position control, compliant tools, and adaptive path planning to maintain stable contact between tool and workpiece.

Compared with traditional fixed-machine polishing, robotic systems offer greater accessibility and flexibility, particularly for sub-aperture processing on strongly curved or highly aspheric zones; however, they face characteristic challenges in stiffness, dynamic accuracy, force stability, vibration suppression, and calibration. Therefore, robotic polishing is most effective when combined with accurate removal-function characterization, robust force control, and frequent metrology feedback—and when its role is clearly positioned within an overall deterministic fabrication chain.

Currently, robotic polishing technology has established mature solutions for processing mirrors with diameters ranging from 1 to 2 meters. Such systems typically employ industrial robots or dedicated manipulators equipped with small polishing tools, achieving stable contact through hybrid force–position control and performing dwell-time compensation based on iterative measurements of surface figure errors and geometric deviations obtained during the process. Typical process configurations include small-tool polishing,[119] bonnet polishing,[120] and magnetorheological finishing (MRF),[121] each of which can be integrated onto a robotic platform to accommodate different curvatures and materials.

In engineering practice, several institutions have applied robotic polishing to the batch production of medium-aperture mirrors. For instance, the Changchun Institute of Optics, Fine Mechanics and Physics (CIOMP) developed a robotic MRF system for 1-meter-class aspheric mirrors, achieving nanometer-level convergence in figure correction.[21, 122] During the fabrication of the ELT secondary mirror (4.25 m diameter), SAGEM-REOSC also employed a dual-head robotic polishing station to accelerate material removal in the rough-polishing stage,[123] although the final figure was still completed using conventional small tools and ion beam figuring. These examples indicate that robotic polishing currently serves mainly the 1–2 m aperture range and is particularly suitable for the serialized and automated production of segmented mirror subunits.

Looking ahead, the trend in robotic polishing lies in higher levels of automation and integration. As demand grows for ultra-large-aperture mirrors ($\geqslant$4 m), a single robot becomes insufficient to cover the entire working surface, making multi-robot collaborative processing a potential technical direction. Through coordinated multi-arm motion, distributed force control, and global figure feedback, it is expected to achieve higher error-correction efficiency and more uniform material removal on large workpieces, thereby shortening the overall manufacturing cycle.

3.4.3 Chapter Summary

The manufacturing equipment system for large-aperture optical mirrors is evolving from isolated processing machines toward integrated closed-loop manufacturing platforms. Future systems will increasingly combine deterministic removal models, in-process sensing, surface-map-driven dwell-time optimization, environmental control, and data-based process compensation. The interplay among these core technological pillars—ranging from ultra-precision machines to system integration—and their associated trends are synthesized in Fig. 28, which moves beyond a tabular listing to provide a schematic overview of the current technological landscape and its future trajectory. Digital twins and artificial-intelligence-based

planning may become useful tools, but their roles should be described as emerging trends unless supported by validated engineering demonstrations.

Overall, the success of large-aperture mirror manufacturing depends on the coordinated development of mirror blank fabrication, surface generation (rough and fine grinding), precision polishing and reliable testing .[124-132] No single technology can independently satisfy all requirements. Instead, the modern fabrication chain relies on hybrid routes that combine efficient generation, controlled grinding, precision polishing and reliable testing.

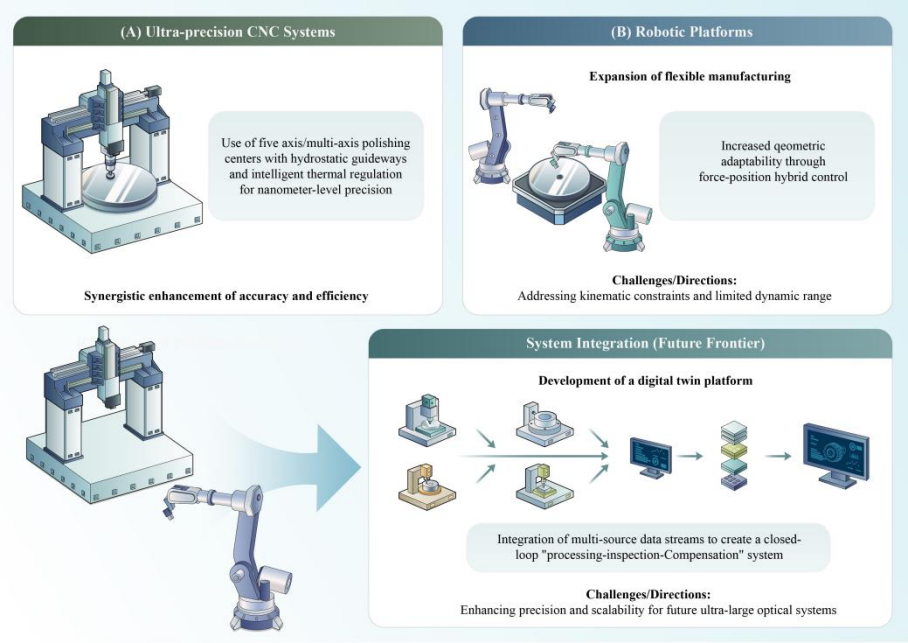

Fig. 27 Schematic overview of large-aperture optical element manufacturing equipment: classification and future trends.

4. Testing of Optical Surfaces During Fabrication

Optical testing is not merely a final verification step; it is an integral part of deterministic fabrication. In the manufacturing of large-aperture mirrors, each round of measurement provides the error map that determines the next material-removal strategy. Therefore, the achievable fabrication accuracy is fundamentally limited by the accuracy, dynamic range, stability, and traceability of the metrology system. Fig. 28 conceptualizes the key role of metrology in the deterministic fabrication loop, mapping predominant testing methods onto the three main mirror production phases:

rough generation, polishing/figuring, and segmented system integration. It illustrates the necessary evolution of metrology from high-dynamic-range profiling to nanometer-sensitive wavefront sensing as the optical surface is refined.

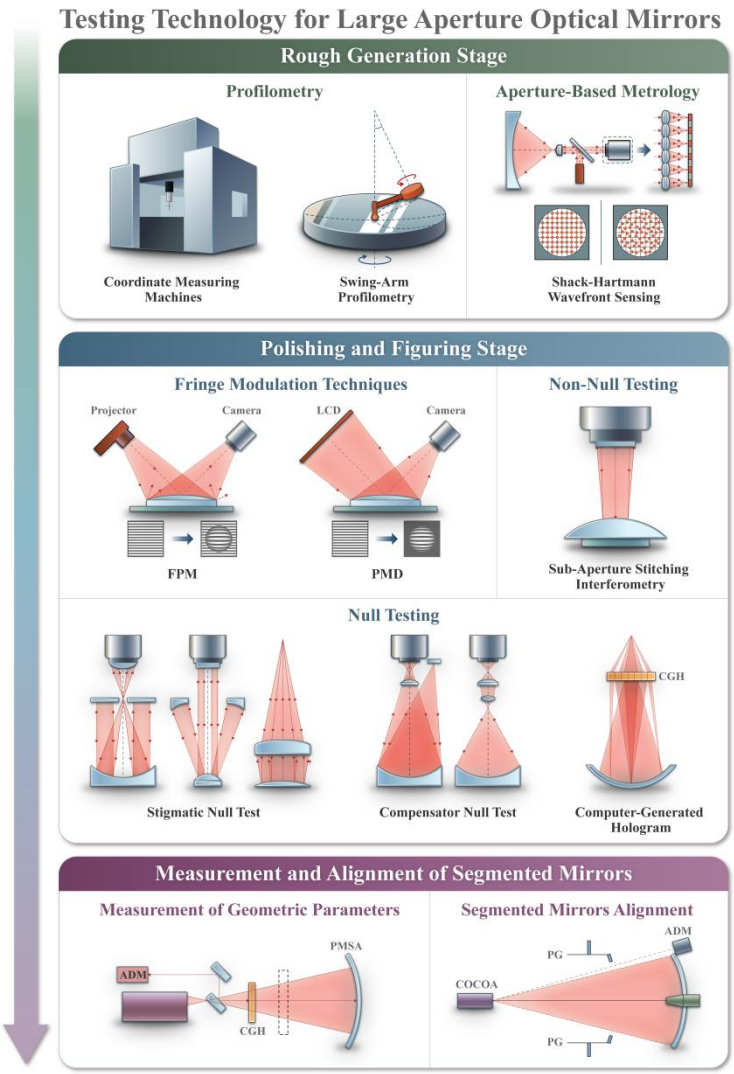

Fig. 28 A panoramic view of testing technologies across the large-aperture mirror manufacturing workflow.

Because the surface condition and accuracy requirement vary substantially across fabrication stages, no single testing method is universally applicable. During rough generation, the surface usually has large figure error, high roughness, and low reflectivity, requiring robust methods with wide dynamic range. During polishing and figuring, the mirror approaches optical quality, and nanometer-level interferometric or wavefront-based methods become essential. For segmented mirrors, additional geometric parameters, such as radius of curvature, segment position, clocking, tilt,

piston, and co-phasing error, must also be measured and controlled.

This section therefore classifies optical testing methods according to their role in the fabrication process: global form measurement in rough generation, high-accuracy surface testing in polishing and figuring, and geometric measurement and alignment for segmented mirrors.

4.1 Rough generation stage: Measuring and controlling the global shape

In the rough generation stage, metrology must tolerate large departures from the nominal surface and must provide sufficiently reliable feedback for subsequent grinding and pre-polishing. The emphasis is not yet final nanometer accuracy, but robust recovery of global form, curvature error, edge tendency, and residual stock distribution. Profilometry, swing-arm profilometry, Shack-Hartmann sensing, and fringe modulation methods are the main techniques used at this stage.

4.1.1 Profilometry and coordinate measurement

Profilometry and coordinate measurement methods (CMM)[133-136] obtain discrete surface coordinates along predefined paths and compare them with the nominal optical prescription. They are particularly useful when the surface is still rough or has a large figure error, where interferometric methods may fail because of insufficient reflectivity or excessive wavefront aberration. A coordinate measuring machine, scanning profilometer, or contact/non-contact displacement sensor can provide micrometer-level surface information over a wide dynamic range.

In large-aperture mirror manufacturing, coordinate metrology is commonly used as an early-stage feedback tool. For example, GTC used large-scale coordinate measurement for its 36 hexagonal primary mirror segments during the grinding phase.[107] JWST used a large Leitz CMM to evaluate the beryllium mirror segments during early fabrication.[137] Similar profilometric approaches were used in the LAMP,[81, 138] Subaru,[60] and ELT[139] projects to verify mirror blanks, polished surfaces, or segment geometries before higher-precision optical testing was introduced.

Fig. 29 Zeiss XENOS series CMM.[140]

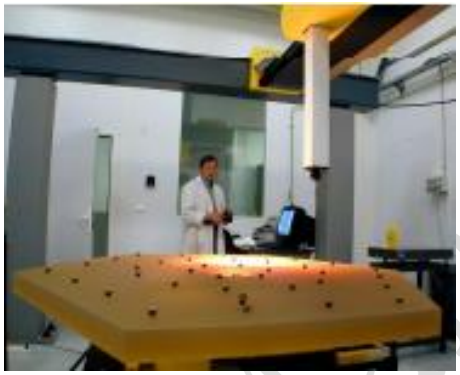

Fig. 30 Large 3D CMM used for GTC mirror segments.[107]

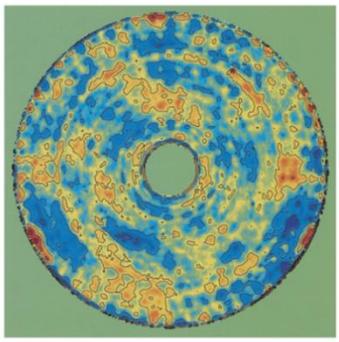

Fig. 31 Surface error map of an 8.2 m primary mirror.[60]

Fig. 32 CMM used in ELT mirror blank measurement.[139]

The main advantage of profilometry is robustness: it is less sensitive to surface reflectivity and roughness than interferometry. Its limitations are measurement time, mechanical positioning error, probe calibration, and sparse sampling. Therefore,

profilometry is best viewed as a global-shape and process-control tool rather than a final acceptance method for optical surfaces.

4.1.2 Swing-arm profilometry

Swing-arm profilometry is a non-contact surface profiling method especially suited to large spherical and aspheric mirrors. The probe arm rotates about a carefully aligned axis so that the sensor follows the best-fit sphere of the test surface, directly measuring departures from that reference. This geometry allows large-aperture surfaces to be measured with high sampling efficiency and a wide dynamic range. [141, 142]

This technique has been adopted in several representative large-mirror projects. The LSST/Rubin secondary mirror was tested using a swing-arm profilometer developed at the University of Arizona. [143] Herschel mirror fabrication also used swing-arm profilometry in the rough processing chain.[144] CIOMP applied a self-developed swing-arm profilometer to the 4.03 m SiC aspheric mirror from grinding to pre-polishing, and the results were consistent with subsequent interferometric measurements.[21]

Swing-arm profilometry is particularly effective for in-process measurement because it can cover large apertures without requiring a full-aperture null test. However, its accuracy depends strongly on rotary-axis calibration, sensor linearity, arm deformation, and error-separation algorithms. It is therefore most powerful when combined with interferometry, CGH testing, or deflectometry in a multi-source metrology strategy.

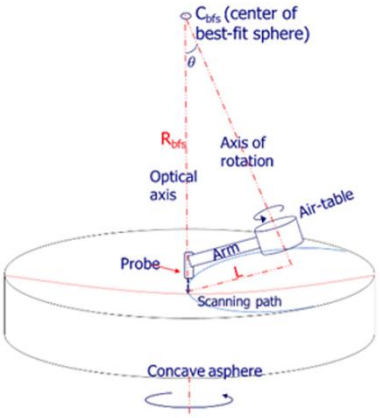

Fig. 33 Swing arm profiler: measuring principle diagram.[145]

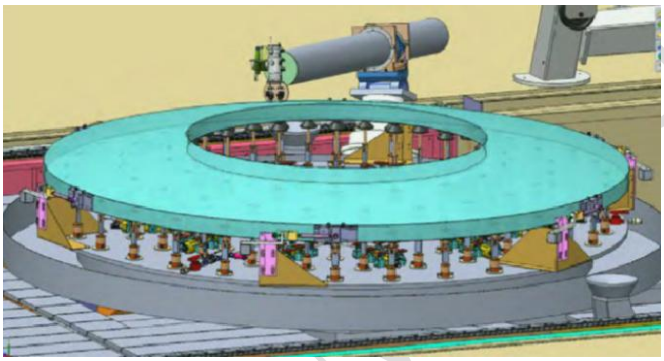

Fig. 34 LSST swing-arm contour meter (SOCMM): inspection schematic.[143]

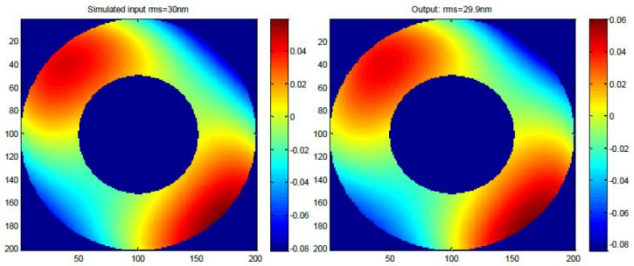

Fig. 35 Simulated SOCMM measurements with 10 nm RMS noise.[116, 143]

Fig. 36 Surface figure characterization of a 4 m aspheric mirror via swing-arm profilometry (SAP) testing. [21]

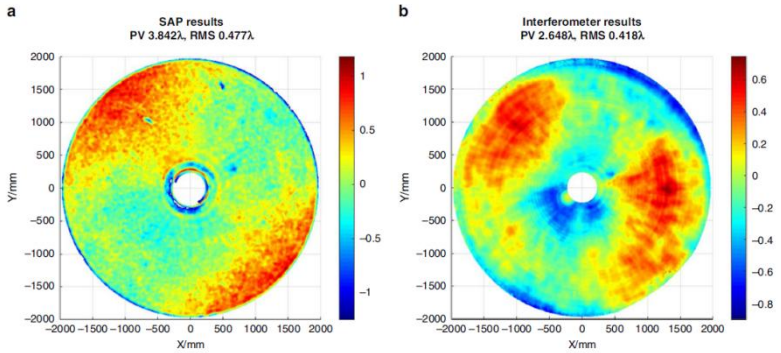

Fig. 37 Surface analysis of 4 m aspheric mirror via SAP testing. [21]

4.1.3 Shack-Hartmann wavefront sensing

Shack-Hartmann wavefront sensing reconstructs surface or wavefront error by measuring local wavefront slopes. Compared with classical Hartmann tests, the use of microlens arrays improves spot localization and enables faster wavefront reconstruction. This method is attractive for rough and intermediate fabrication stages because it is non-contact, relatively simple in optical configuration, and capable of acquiring large-area slope information efficiently.

In large telescope manufacturing, Shack-Hartmann or scanning Shack-Hartmann methods have been used as practical tools for characterizing wavefront and mid-spatial-frequency errors. JWST mirror fabrication, for example, used an infrared scanning Shack-Hartmann sensor variant to evaluate segment errors at intermediate stages.[134] In other projects, Shack-Hartmann methods have served as complementary metrology to profilometry and interferometry.

Its main limitations arise from microlens aperture, spatial sampling density, calibration, and reconstruction error.[87, 114, 146, 147] As a result, Shack-Hartmann sensing is most useful as a rapid slope-based measurement method rather than a universal replacement for high-accuracy interferometry.

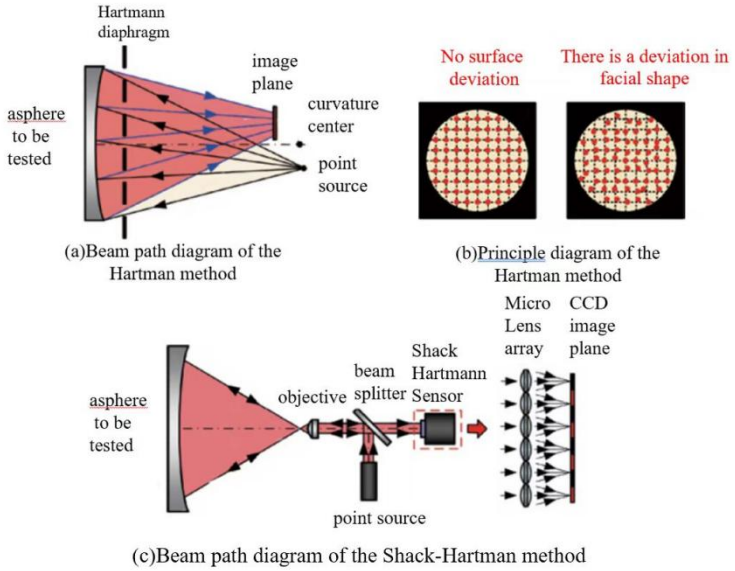

Fig. 38 Principle schematics and measurement results of Hartmann and Shack–Hartmann wavefront sensing methods.[43]

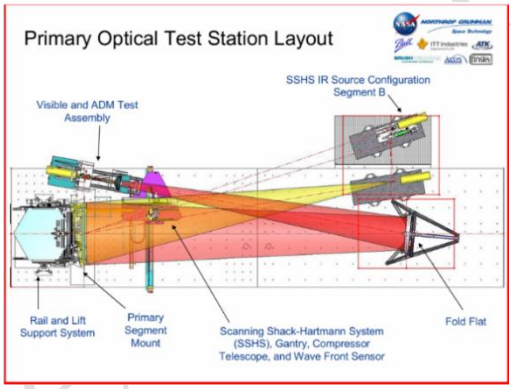

Fig. 39 Optical layout schematic of the SSHS.[43]

4.1.4 Fringe modulation and phase measuring deflectometry

Fringe modulation methods, including structured light, Ronchi testing, and phase measuring deflectometry, infer surface shape from the deformation of projected or reflected fringe patterns.[148, 149] For specular optical surfaces, phase measuring deflectometry is particularly useful because it measures slope information with a large dynamic range and relatively simple hardware.[150]

The SCOTS system developed at the University of Arizona is a representative implementation of this idea. It has been used to test large off-axis aspheric mirrors, including GMT segments, where its results showed good agreement with interferometric measurements after calibration and correction. Similar deflectometric

approaches are increasingly used as complementary tools for complex aspheres whose slope range exceeds that of conventional interferometric setups.[151, 152]

The strength of fringe modulation methods lies in their large dynamic range, non-contact operation, and suitability for difficult aspheric surfaces. Their limitations include calibration sensitivity, coordinate-system reconstruction, iterative computation, and dependence on accurate geometric modeling. Therefore, they are often used in combination with interferometry rather than as an isolated final test. The fringe modulation technology is also constantly evolving. In recent years, it has been deeply explored in areas such as the integration with deep learning,[153-155] projection systems,[156] Phase retrieval,[157] encoding and labeling,[158] defocus measurement,[159] and 3D reconstruction.[155]

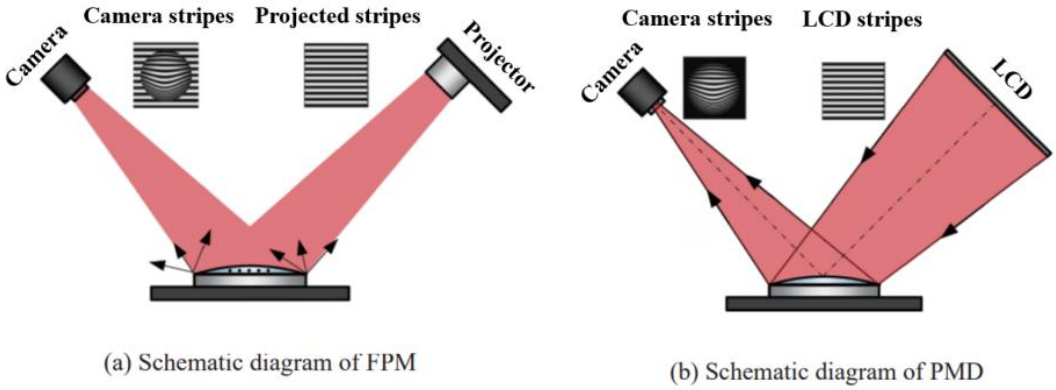

Fig. 40 Schematic of structured light methods.[130]

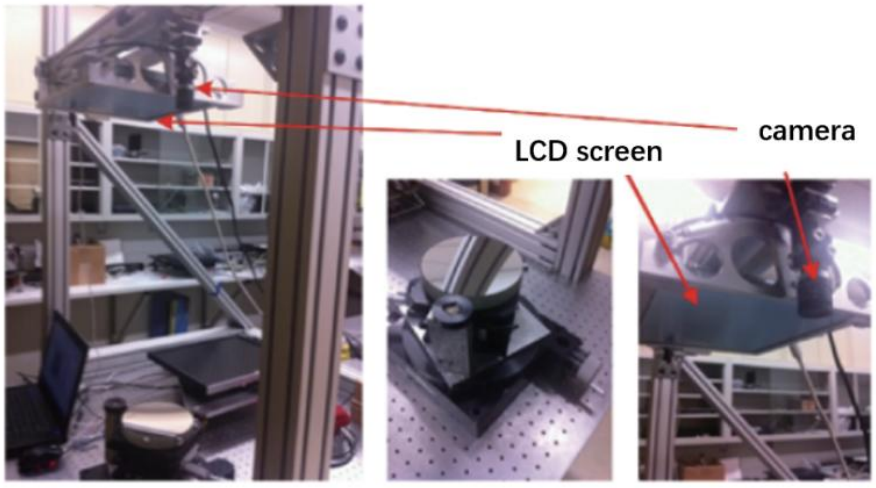

Fig. 41 Optical layout of the SCOTS system.[152]

4.2 Polishing and figuring stage: Measuring and perfecting the surface

Once polishing and deterministic figuring begin, surface errors must be reduced to the nanometer scale. At this stage, interferometric techniques become the main metrology route. Depending on whether the nominal aspheric aberration is optically compensated, these techniques can be divided into non-null and null testing methods.

4.2.1 Non-null testing: sub-aperture stitching interferometry

Sub-aperture stitching interferometry measures a large mirror by dividing it into smaller overlapping regions and reconstructing the full-aperture surface through stitching algorithms. This method avoids the need for a single full-aperture reference optic and is therefore highly valuable for large convex aspheres and mirrors whose size exceeds available interferometric test optics.[160-163]

Representative applications include the LSST/Rubin secondary mirror, where sub-aperture Fizeau testing was used to reconstruct the full-aperture surface;[164, 165] the TMT secondary mirror, where multiple off-axis aspheric test plates were proposed to deal with the absence of a central aperture;[165] and the ELT M2 mirror, where sectorial sub-aperture stitching was used for the 4.25 m convex aspheric surface.[109, 166]

The method offers high accuracy and strong adaptability, but its performance is limited by stage positioning, overlap accuracy, systematic error coupling, environmental stability, and stitching algorithm robustness. For this reason, modern stitching interferometry increasingly relies on calibrated motion systems, redundant overlap strategies, and uncertainty analysis.[167-175]

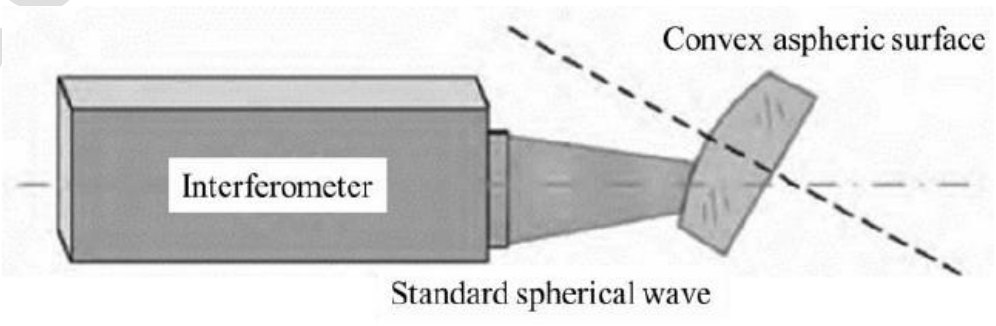

Fig. 42 Schematic of sub-aperture stitching interferometry.[160]

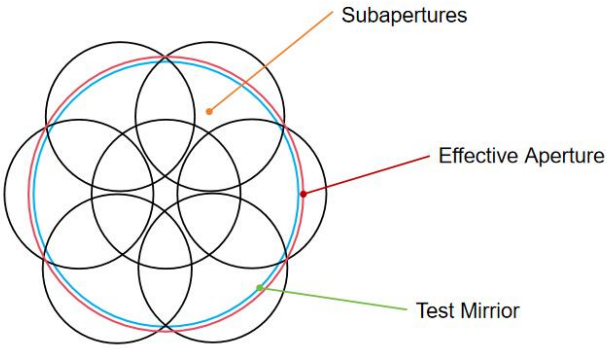

Fig. 43 Schematic of the circular sub-aperture layout.

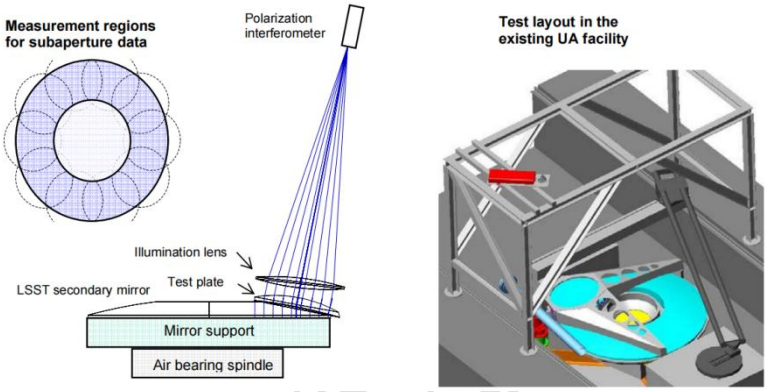

Fig. 44 Layout for LSST secondary mirror test in the Optical Sciences shop at the University of Arizona.[165]

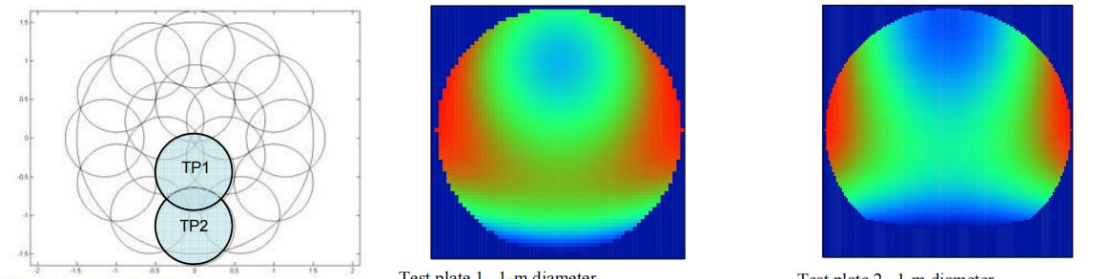

Fig. 45 Layout and aspheric departure of test plates for the Fizeau test of the TMT secondary mirror.[165]

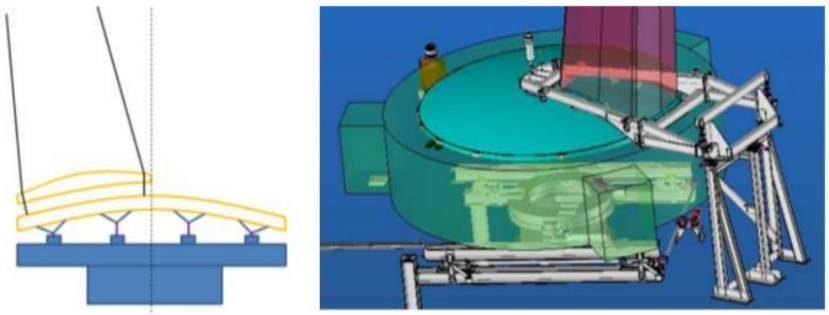

Fig. 46 ELT M2 test bench concept at Safran REOSC. An aspheric reference plate is used for sub-aperture Fizeau testing.[109]

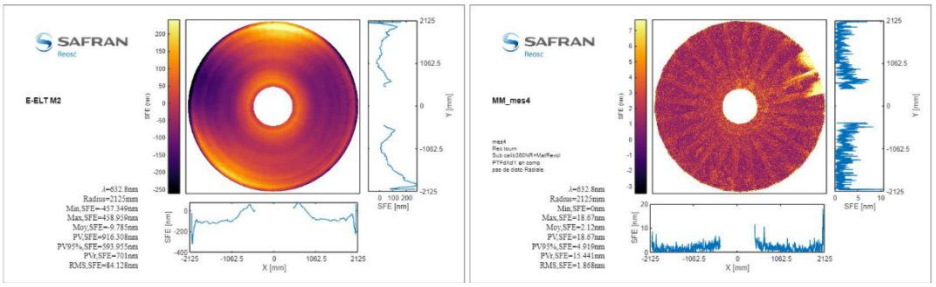

Fig. 47 ELT M2 surface figure error map after six polishing iterations/mismatch map obtained after stitching.[166]

4.2.2 Null testing: stigmatic, compensator, and CGH methods

Null testing converts the ideal reflected wavefront of an aspheric surface into a plane or spherical wave so that residual fringes directly represent surface error. It is the dominant approach for high-precision polishing-stage and final testing of large optical mirrors.

4.2.2.1 Stigmatic null test

Stigmatic null tests use the conjugate-point property of conic surfaces and can achieve very high accuracy for suitable quadric mirrors. The classical Hindle test and its variants belong to this category. These methods are optically elegant and accurate, but they usually require large, high-quality auxiliary optics and precise alignment.[26, 176]

For segmented mirrors, related null or autocollimation configurations have been used to test individual segments. Keck, for instance, employed interferometric folded autocollimation testing during the fine polishing of its hexagonal segments.[4, 26, 74, 104, 177, 178] This illustrates the role of stigmatic or near-stigmatic null concepts in segment-level verification.

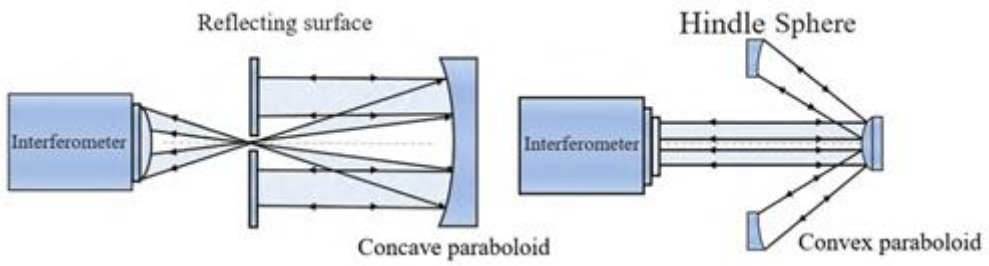

Fig. 48 Stigmatic null test optical path.[176]

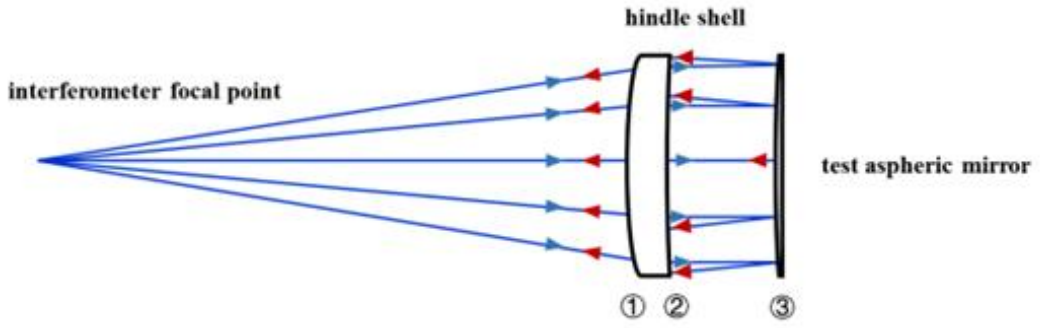

Fig. 49 Hindle shell interference compensation test optical path.[176]

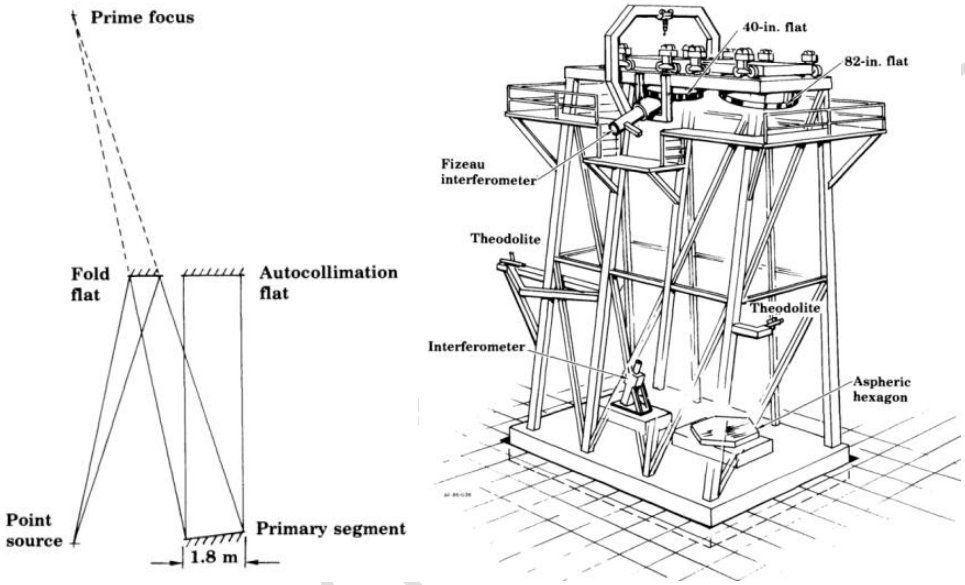

Fig. 50 (a) Folded autocollimation test and (b) autocollimation test facility.[179]

4.2.2.2 Compensator null test

Compensator null tests use refractive or reflective optics to compensate the nominal aberration of an aspheric mirror.[180] Dall[181] and Offner[182] compensators are common examples. This approach is suitable for rotationally symmetric aspheres and has long been a standard method for high-precision testing of large telescope mirrors.

Several flagship projects demonstrate its importance. The Hubble Space Telescope primary mirror used a reflective null compensator, although the well-known testing error in that project also became a historical reminder that null-test calibration and independent verification are essential.[181, 183-186] Gemini used infrared and visible-light null compensators at different fabrication stages.[187-189] LSST/Rubin M1 was tested using an Offner null compensator, with CGH-based

verification of the compensator.[2, 106]

The method provides high accuracy but is limited by compensator design, fabrication, alignment sensitivity, and lack of universality. For convex or highly aspheric surfaces, the required auxiliary optics can become large or difficult to manufacture, motivating the use of CGH-assisted, partial-null, or stitching-based configurations.

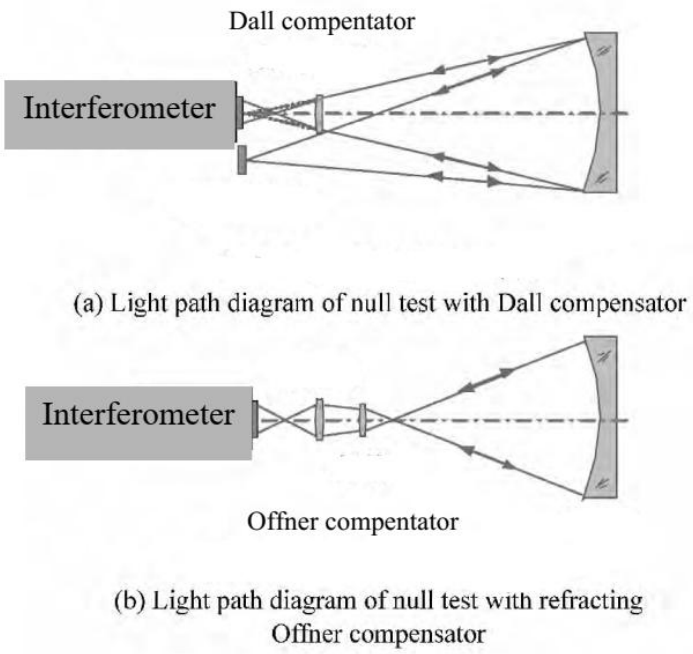

Fig. 51 Optical path diagrams for testing aspheric surfaces using the compensator mirror method.[190]

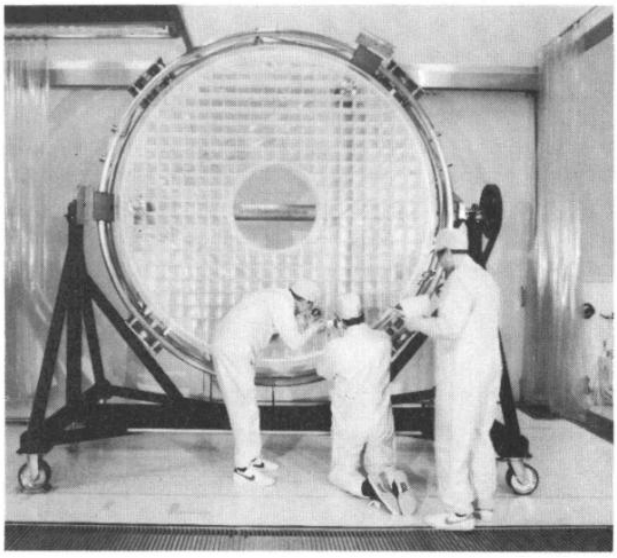

Fig. 52 Primary mirror of the Hubble Space Telescope.[183]

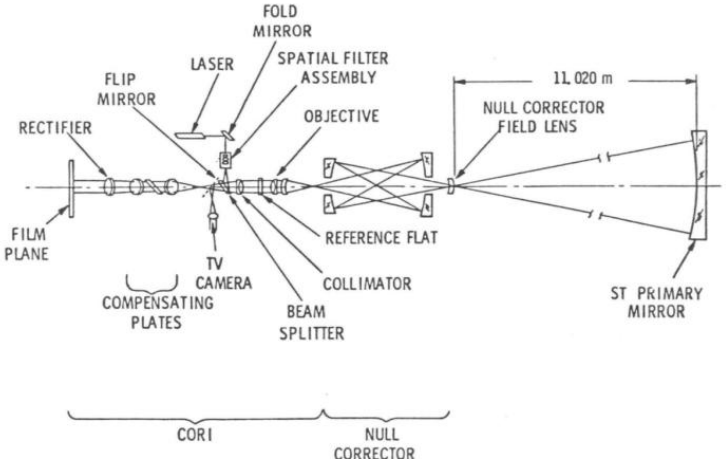

Fig. 53 Test optical path for the Hubble Space Telescope primary mirror.[183]

Fig. 54 Interferogram of the Gemini primary mirror testing.[189]

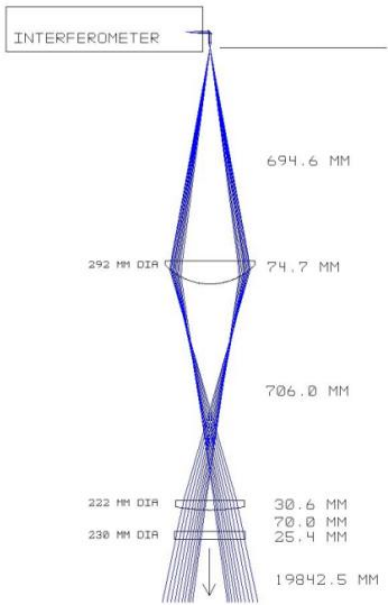

Fig. 55 Null corrector layout for M1 (two-element Offner).[2]

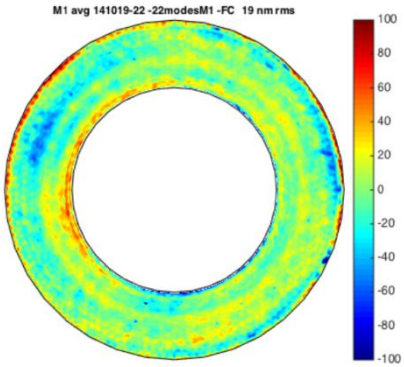

Fig. 56 Surface Figure Error Map of M1.[106]

4.2.2.3 CGH testing

Computer-generated hologram testing uses diffractive structures to generate the desired reference wavefront for an aspheric or freeform surface. Compared with conventional compensators, CGHs can encode complex wavefronts and alignment features, making them particularly suitable for large aspheres, off-axis mirrors, and segmented mirror elements.[191]

CGH[192] testing has been widely adopted in major projects. SDSS used CGH-assisted interferometry to simplify testing of convex aspheric components. GTC used CGH testing in its segment fabrication and global evaluation process.[105] LSST/Rubin used CGH testing for M3 and for verification of null configurations.[192] GMT segment testing employed CGH-based null interferometry for large off-axis segments.[193] Seimei used CGH real-time testing in segment fabrication[61, 194], while CIOMP combined CGH null testing with swing-arm profilometry and phase-shifting deflectometry for the 4.03 m SiC mirror.

CGH testing has become one of the most versatile high-precision methods for modern large-aperture optical fabrication.[195-201] Its limitations are mainly associated with CGH fabrication error, diffraction-order management, alignment sensitivity, substrate error, and absolute calibration. Consequently, CGH testing is most reliable when supported by independent verification, error budgeting, and cross-checking with other metrology methods.

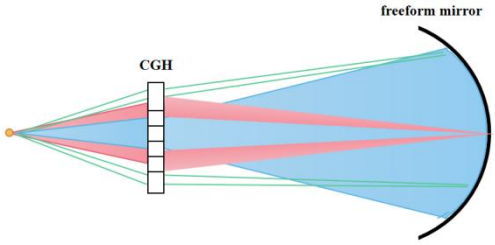

Fig. 57 Schematic of the CGH testing principle.

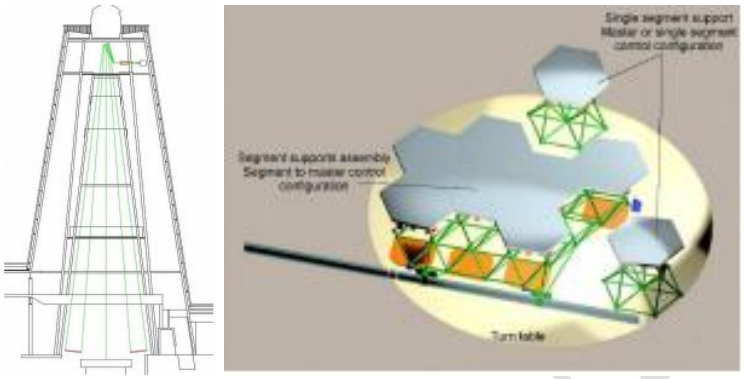

Fig. 58 (a) 29 m-high test tower and global test platform; (b) schematic of mirror segment assembly.[105, 108]

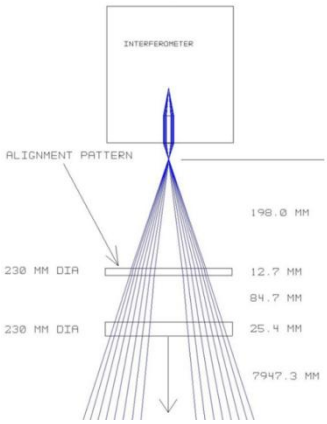

Fig. 59 CGH test configuration for M3.[192]

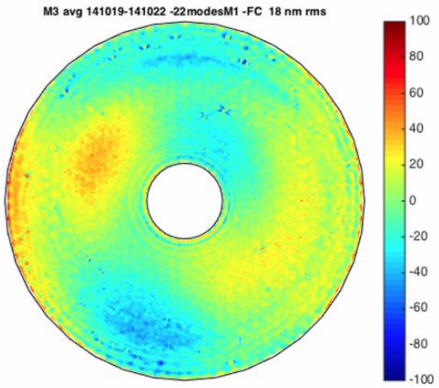

Fig. 60 Residual surface figure of M3 following active optics correction.[137]

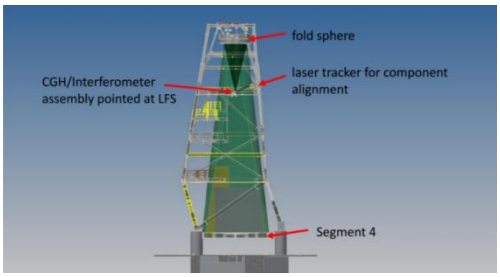

Fig. 61 GMT primary mirror is tested inside a 28 m test facility.[75]

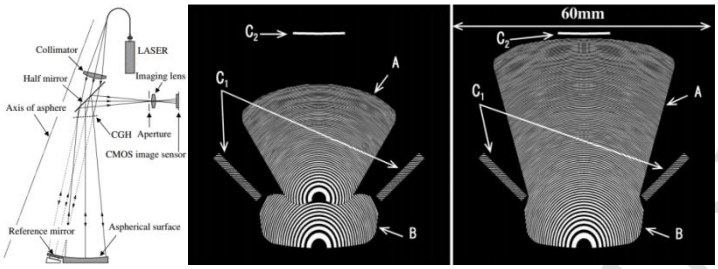

Fig. 62 CGH splits the incident beam into a test beam and a reference beam (left); CGH pattern (right).[202]

4.3 Geometric parameter measurement and alignment of segmented mirrors

For segmented mirrors, surface figure testing alone is insufficient. Each segment must also satisfy geometric and assembly requirements, including radius of curvature, segment position, tilt, clocking, piston, edge matching, and co-phasing. These parameters determine whether independently fabricated segments can form an equivalent continuous aperture.

Radius-of-curvature control is a representative example. In JWST, each beryllium segment was equipped with a RoC actuation system, but excessive correction would introduce residual surface error. Therefore, accurate RoC measurement using interferometry, CGH, absolute distance measurement, and calibration optics was essential for reducing the burden on active correction.[21]

Alignment and co-phasing require a staged strategy. JWST used photogrammetry for coarse segment positioning, center-of-curvature optical measurements for intermediate alignment, and multi-wavelength interferometric correction for fine phasing. Large ground-based segmented telescopes such as ELT and TMT extend the same principle to hundreds of segments, requiring robust segment-level metrology, actuator calibration, and wavefront control.[203, 204]

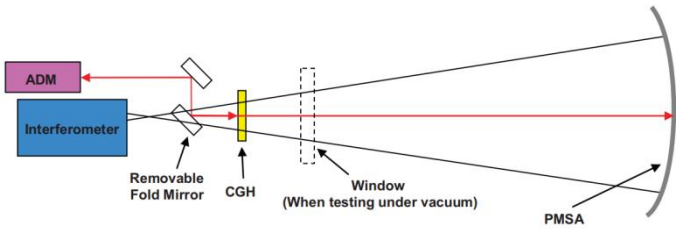

Fig. 63 Schematic of the RoC measurement system.[21]

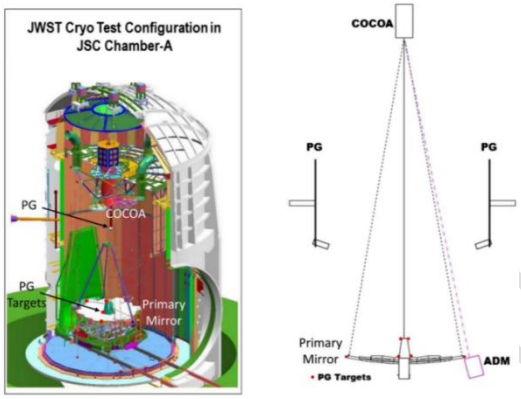

Fig. 64 Model and schematic of the test setup.[205]

4.4 Chapter Summary

The testing methods used in large-aperture mirror fabrication form a staged and complementary system. Rough-stage methods provide wide dynamic range and robustness; polishing-stage methods provide nanometer-scale sensitivity; segmented-mirror methods add geometric consistency and co-phasing control. The most successful projects do not rely on a single method, but on cross-validated metrology chains that connect fabrication, measurement, correction, and acceptance.

In a complete manufacturing flow, a large-aperture optical mirror typically undergoes stages from milling/grinding, loose-abrasive grinding, polishing, and figure finishing, to iterative metrology and final acceptance. Fig. 65 consolidates the staged and complementary nature of optical testing into a hierarchical framework. It should be noted that this schematic primarily synthesizes representative cases and technologies from the open literature, as reviewed in this article. Due to limitations in publicly disclosed information and the review's focus on key technologies, the following figures showcase specific projects and associated techniques discussed herein. This framework visually affirms the principle that no single method is

sufficient; rather, a cross-validated metrology chain-encompassing techniques from laser/photogrammetry for large-scale form to interferometry and profilometry for nano-scale finish-must evolve in lockstep with the workpiece's surface condition.

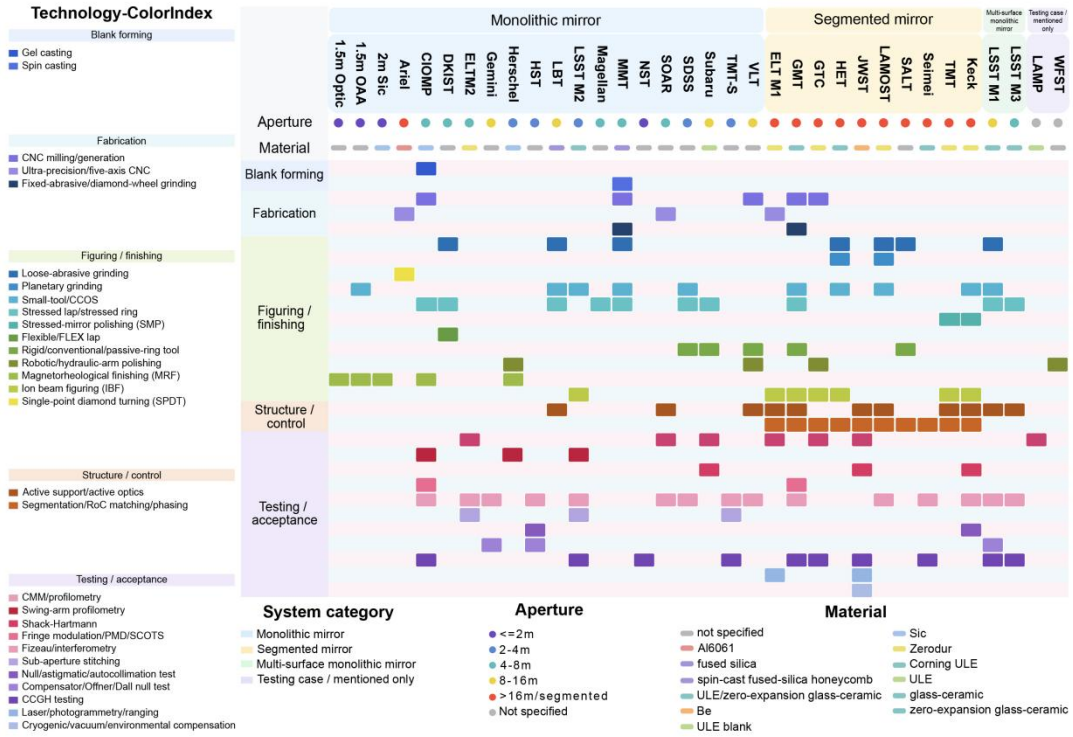

Fig. 65 A technology-method heatmap for manufacturing and testing monolithic vs. segmented mirrors.

5. Performance Parameters and Acceptance Criteria for Large-Aperture Optical Mirrors

Acceptance of large-aperture optical mirrors is a system-level verification process. It cannot be reduced to a single surface figure value, because mirror performance depends simultaneously on optical accuracy, structural stability, thermal behavior, environmental adaptability, coating quality, support conditions, and metrology uncertainty. The acceptance framework must therefore connect the fabricated mirror surface with the scientific requirements of the telescope.

The acceptance criteria also differ across platforms. Ground-based telescopes emphasize gravity deformation, wind load, thermal gradients, seismic disturbance, maintainability, and active optics compatibility. Space telescopes place greater

emphasis on lightweighting, launch vibration, vacuum compatibility, cryogenic stability, deployment accuracy, contamination control, and on-orbit wavefront performance. Segmented mirrors add further requirements on segment-to-segment consistency, radius of curvature, edge quality, and phasing capability.

5.1 Key parameters and acceptance criteria

The first category is optical performance. Surface figure error, wavefront error, roughness, mid-spatial-frequency error, and power spectral density are the principal optical indicators. Projects such as LSST/Rubin,[47, 60, 80] Gemini,[188, 189] Subaru,[8] LBT,[25, 58, 82] and CIOMP's 4.03 m SiC mirror[21] demonstrate that nanometer-level RMS surface accuracy can be achieved through closed-loop polishing and high-precision testing. For segmented telescopes such as Keck,[4, 73, 74] JWST,[20, 43, 203] ELT,[14, 35, 111, 206, 207] and TMT,[208] the same optical indicators must be evaluated at both segment and system levels.

The second category is geometric consistency. For segmented mirrors, radius-of-curvature variation, edge roll-off, segment shape repeatability, actuator interface position, and co-phasing error directly affect the global wavefront. JWST provides a typical example: although each segment has a RoC actuation mechanism, excessive RoC correction introduces residual figure error, so segment-to-segment RoC consistency must be controlled during fabrication and acceptance.

The third category is mechanical and support performance. Large mirrors deform under gravity, support force error, temperature change, and handling loads. Subaru and LSST/Rubin illustrate the importance of carefully designed passive or active support systems for maintaining surface figure. ELT and TMT further extend this requirement to hundreds of supported segments, where support pad bonding, actuator stiffness, and structural repeatability become part of the acceptance problem.

The fourth category is environmental adaptability. Space telescopes such as JWST and Herschel require verification under vacuum, cryogenic, and launch-load conditions.[43, 209] Ground-based extremely large telescopes such as ELT[109, 207] and TMT

must consider wind buffeting, seismic disturbance, dome seeing, temperature gradients, and long-term structural stability. Therefore, environmental testing and finite-element-based prediction must be linked to optical acceptance.

Table 7 Summary of Technical Requirements for Optical Surface Quality

Acceptance category	Main parameters	Representative project emphasis
Optical surface quality	Surface figure error, wavefront error, RMS/PV, roughness, PSD, mid-spatial-frequency error.	LSST/Rubin, Gemini, Subaru, LBT, CIOMP 4.03 m SiC mirror.
Segment consistency	RoC consistency, edge roll-off, actuator interface accuracy, phasing margin, segment-to-segment matching.	Keck, JWST, GTC, ELT, TMT, GMT.
Mechanical stability	Gravity deformation, support force accuracy, stiffness, handling deformation, long-term repeatability.	Subaru support system, LSST/Rubin active support, ELT/TMT segment support systems.
Thermal stability	CTE, thermal gradient sensitivity, thermal conductivity, cryogenic deformation, thermo-elastic coupling.	JWST cryogenic beryllium mirrors, Herschel SiC mirror, ULE/Zerodur ground-based mirrors.
Environmental adaptability	Vacuum compatibility, launch vibration, wind load, seismic load, contamination, coating stability.	JWST and Herschel for space environments; ELT and TMT for ground-based environmental loading.
Metrology traceability	Calibration chain, uncertainty budget, cross-validation, repeatability and reproducibility.	Hubble as a historical warning; CGH/compensator/stitching cross-checks in LSST/Rubin, GTC, ELT, and CIOMP projects.

5.2 Key issues in the implementation of the acceptance process

A major challenge is the lack of universal acceptance criteria across telescope types. A metric that is decisive for a cryogenic space telescope may not be the limiting factor for a ground-based active-optics system, and vice versa. Therefore, acceptance specifications must be derived from scientific objectives, optical design, operational environment, and correction capability rather than copied directly from previous projects.

A second issue is the uncertainty of large-scale optical testing. For large mirrors, the test system itself may require custom null optics, large mechanical stages, CGHs, stitching algorithms, or environmental control. The Hubble primary mirror demonstrated the consequences of relying on an insufficiently verified null test.

Modern projects therefore emphasize independent cross-checks, calibration optics, test-system error budgeting, and traceability to reduce systematic error.

A third issue is environmental interference during testing. Atmospheric turbulence, vibration, acoustic disturbance, and temperature drift can distort ground-based measurements. For space mirrors, cryogenic vacuum testing introduces long-term stability and thermal compensation requirements. Projects such as JWST, LSST/Rubin, and ELT show that acceptance testing must be treated as a coupled optical-mechanical-thermal problem.[210]

A fourth issue is the scalability of acceptance. Segmented telescopes require repeatable verification for dozens, hundreds, or even more than one thousand mirror elements and interfaces. Acceptance must therefore evolve from one-off testing toward standardized, semi-automated, traceable, and statistically controlled processes.

6. Summary and Outlook

The manufacturing and testing of large-aperture optical mirrors have evolved from experience-based craft processes toward deterministic, model-driven, and metrology-guided engineering systems. In manufacturing[211-216], large-scale CNC generation, stressed-lap, small-tool, MRF, IBF, and robotic manufacturing methods now form complementary process chains. In testing[168, 217-222], swing-arm profilometry, Shack-Hartmann sensing, deflectometry, sub-aperture stitching interferometry, compensator null testing, and CGH testing provide staged feedback from rough generation to final acceptance.

Representative projects reveal the logic of this evolution. Keck and GTC demonstrated the feasibility of segmented primary mirrors and established important segment fabrication and testing routes. Subaru, VLT, LBT, SOAR, and LSST/Rubin advanced large monolithic and integrated-mirror fabrication through deterministic polishing and high-precision null testing. JWST extended segmented mirror technology into cryogenic space operation, requiring lightweight materials,

deployment control, and wavefront sensing. ELT, TMT, and GMT push the field toward industrial-scale production of large off-axis or segmented optics. CIOMP's 4.03 m SiC mirror demonstrates the importance of integrating mirror blank preparation, deterministic polishing, and multi-source testing for large SiC optics.

Despite these advances, important bottlenecks remain. Large monolithic mirrors are constrained by blank fabrication, transport, gravity deformation, thermal management, and full-aperture testing. Segmented mirrors face challenges in batch consistency, edge control, co-phasing, actuator integration, and production throughput. Deterministic figuring techniques such as MRF and IBF provide high accuracy, but their efficiency, stability, thermal effects, and scalability still require improvement. Metrology systems must also address uncertainty accumulation, environmental disturbance, and the need for cross-validation among different testing principles.

Artificial intelligence, digital twins, and data-driven optimization are increasingly being explored across the entire optical manufacturing and testing chain. On the manufacturing side, these techniques are being applied to various stages, from rough grinding to deterministic polishing processes such as stressed-lap, small-tool , MRF, IBF and so on. On the testing side, they are being integrated into CMM measurement, Shack-Hartmann wavefront reconstruction, fringe modulation analysis, sub-aperture stitching, compensator null testing, and CGH error calibration. At present, however, many of these studies remain at the algorithmic or laboratory-demonstration stage. They should therefore be described as emerging directions rather than mature replacements for physics-based process control.

Table 8 outlines a comprehensive roadmap for the evolution of optical manufacturing and testing, driven by the demands of next-generation large-aperture telescopes. A central theme is the relentless pursuit of extreme precision, pushing fabrication toward nanoscale and sub-nanoscale surface accuracy while imposing more stringent measurement requirements on testing technologies to ensure the accurate characterization of manufacturing results. This is coupled with a decisive

shift from contact-based methods, rather favoring non-contact energy-field polishing for near-defect-free manufacturing and non-contact testing techniques like interferometry for damage-free measurement. Furthermore, the entire ecosystem is moving towards greater intelligence and automation, with AI-driven, closed-loop "processing–inspection" chains and digital twins that will enhance efficiency and precision. The paradigm is expanding beyond terrestrial limits, with ambitious research focused on intelligent full-chain manufacturing and the groundbreaking potential of in-orbit manufacturing and testing to overcome the constraints of Earth's gravity.

Table 8 Trends in Optical Manufacturing and Testing for Large-Aperture Telescopes

Domain	Core Trend / Direction	Key Details and Technologies
Current manufacturing trends	Extreme surface accuracy	Pursuing nanoscale shape accuracy on complex surfaces and sub-nanoscale super-smooth surfaces
	Non-Destructive fabrication	Future efforts should focus on reducing workpiece surface/subsurface damage in conventional contact processes, while also developing new principles such as non-contact energy-field polishing for near-defect-free manufacturing.
	High-efficiency and automated production	Improving mass production efficiency, equipment reliability/flexibility, and implementing intelligent fabrication for rapid-response capability
Current testing trends	Nanometer-level testing accuracy	Requiring advanced interferometers, CGHs, stitching techniques, and sophisticated data processing algorithms for nanometer/sub-nanometer accuracy
	Non-contact testing as mainstream	Utilizing principles like optical interference and laser scattering for fast, accurate, and damage-free measurement of topography, roughness, and defects
System integration	Intelligent systems	Integrating smart sensors, computational imaging, and AI to enable autonomous closed-loop control throughout the fabrication chain, enhancing efficiency and accuracy
Future innovation directions	Intelligent full-chain manufacturing	Developing an AI-driven "processing–inspection" loop, incorporating digital twins and multi-physics simulations to improve efficiency and precision
	In-orbit manufacturing and testing paradigms	Designing polishing systems for zero-gravity environments to overcome terrestrial deformation limits, combined with in-situ space testing technologies (e.g., coherent diffraction imaging)

In conclusion, large-aperture optical mirror technology is advancing toward higher precision, larger scale, stronger process integration, and more intelligent closed-loop control. Manufacturing and testing are no longer separable activities: fabrication depends on metrology feedback, while metrology requirements are defined by fabrication strategy and system performance. The next generation of ground-based

and space-based observatories will therefore depend on the coordinated progress of materials, structural design, deterministic manufacturing, optical testing, active control, and acceptance methodology.

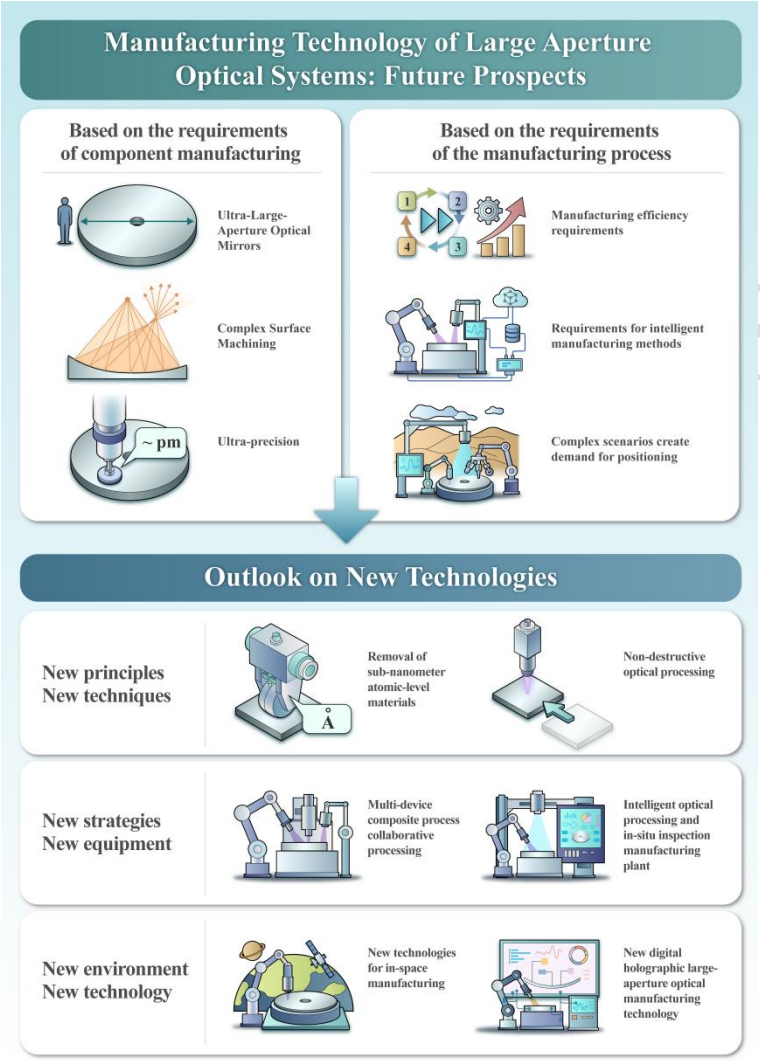

Fig. 66 A system-level framework for the future of large-aperture optical manufacturing.

Acknowledgments

We acknowledge the financial support of the Project supported by the State Administration for Science, Technology and Industry for National Defense (JSZL2023130B001); Project supported by Jilin Province Development and Reform Commission (2024C001); National Natural Science Foundation of China (Grant No. 62275246); National Natural Science Foundation of China (Grant No. 62305334).

Figure Permissions:

All SPIE figures are reprinted with permission from SPIE. Reproduced with permission. Fig. 62 is reprinted with permission from Ref. [203], © Optica Publishing Group. All other figures are reproduced from open-access sources under applicable Creative Commons licenses or publisher permissions, with proper attribution provided in the respective figure captions.

Author Contributions

Conceptualization, Supervision, Funding acquisition: Xuejun Zhang(lead), Longxiang Li(equal), Qiang Cheng(equal), Donglin Xue(equal). **Formal analysis, Resources, Methodology:** Xuejun Zhang(lead), Longxiang Li(equal), Qiang Cheng(equal). **Investigation:** Longxiang Li(lead), Ximing Liu(equal), Yunfan Yang(equal), Hongshi Li(equal), Runmu Cheng(equal). **Project administration:** Longxiang Li(lead), Qiang Cheng(equal). **Validation:** Xuejun Zhang(lead), Longxiang Li(equal). **Visualization, Data curation, Writing-original draft, review & editing:** Longxiang Li(lead), Ximing Liu(equal), Yunfan Yang(equal), Hongshi Li(equal).

Conflict of Interest

The authors declare no competing interests.

Supplementary Information

Supplementary materials are available in the online version.

References

1. Tuell, M.T. et al.Fabrication of the LSST monolithic primary-tertiary mirror.SPIE Astronomical Telescopes + Instrumentation. **8450**, 1531-1546 (2012).

2. Araujo-Hauck, C. et al.LSST mirror system status: from design to fabrication and integration.SPIE Astronomical Telescopes + Instrumentation. **9906**, 202-211 (2016).

3. Ioannisiani, B.K. et al. The Zelenchuk 6m Telescope (BTA) of the USSR Academy of Sciences. International Astronomical Union Colloquium **67**, 3-9

(1982).

4. Allen, L.N. et al.Surface error correction of a Keck 10-m telescope primary mirror segment by ion figuring.San Diego, '91. **1531**, 195-204 (1992).

5. Barnes III, T.G. et al.Commissioning experience with the 9.2-m Hobby-Eberly Telescope.Astronomical Telescopes and Instrumentation. **4004**, 14-25 (2000).

6. Cayrel, M.Completion of VLT and GEMINI primary mirrors at REOSC.Astronomical Telescopes and Instrumentation. **4003**, 14-23 (2000).

7. Stobie, R., Meiring, J.G. & Buckley, D.A.Design of the southern African large telescope (SALT).Astronomical Telescopes and Instrumentation. **4003**, 355-362 (2000).

8. Iye, M. et al. Current performance and on-going improvements of the 8.2 m Subaru Telescope. Publications of the Astronomical Society of Japan **56**, 381-397 (2004).

9. Neufeld, C. et al.The active primary mirror assembly for the SOAR telescope.SPIE Astronomical Telescopes + Instrumentation. **5489**, 870-880 (2004).

10. Alvarez, P., López-Tarruella, J.C. & Rodriguez-Espinosa, J.The GTC project: preparing the first light.SPIE Astronomical Telescopes + Instrumentation. **6267**, 70-79 (2006).

11. Hill, J.M. The large binocular telescope. Applied Optics **49**, D115-D122 (2010).

12. Johns, M. et al.Giant magellan telescope: overview.SPIE Astronomical Telescopes + Instrumentation. **8444**, 526-541 (2012).

13. McMullin, J.P. et al.The Advanced Technology Solar Telescope: Design and Early Construction.SPIE Astronomical Telescopes + Instrumentation. **8444**, 41-52 (2012).

14. Bourgois, R. et al.ELT optics polishing: year 1 report.SPIE Astronomical Telescopes + Instrumentation. **10706**, 246-255 (2018).

15. Kudryavtsev, D.O. & Vlasyuk, V.V. The Largest Russian Optical Telescope BTA: Current Status and Modernization Prospects. arXiv preprint

arXiv:2012.08754 (2020).

16. Liu, Z. et al. Introduction to the Chinese Giant Solar Telescope (SPIE, 2012).

17. McMullin, J. et al. The Advanced Technology Solar Telescope: design and early construction (SPIE, 2012).

18. Bourgois, R. et al. ELT optics polishing: year 1 report (SPIE, 2018).

19. Korhonen, T. et al.Polishing and testing of the 3.5 m SiC M1 mirror of the Herschel space observatory of ESA.Optical Systems Design. **7102**, 423-429 (2008).

20. Stahl, H.P.JWST mirror technology development results.Optical Engineering + Applications. **6671**, 11-22 (2007).

21. Zhang, X. et al. Challenges and strategies in high-accuracy manufacturing of the world's largest SiC aspheric mirror. Light: Science & Applications **11**, 310 (2022).

22. Zhang, G. Gelcasting process of 1.5 m SiC ceramic green body. Opt. Precision Eng **21**, 2989-2993 (2013).

23. Bai, Y. et al. Material removal model of magnetorheological finishing based on dense granular flow theory. Light: Advanced Manufacturing **3**, 630-639 (2022).

24. Hu, H. et al. Designing a hydraulic support system for large monolithic mirror's precise in-situ testing-polishing iteration. Optics Express **27**, 3746-3760 (2019).

25. Hill, J.M. & Salinari, P.The large binocular telescope project.SPIE Astronomical Telescopes + Instrumentation. **5489**, 603-614 (2004).

26. Nelson, J. & Mast, T.Construction of the Keck Observatory.SPIE Astronomical Telescopes and Instrumentation for the 21st Century. **1236**, 47-55 (1990).

27. Bos, A. et al. Nanometre-accurate form measurement machine for E-ELT M1 segments. **40**, 14-25 (2015).

28. Tuell, M.T. et al.Final acceptance testing of the LSST monolithic primary/tertiary mirror.Advances in Optical and Mechanical Technologies for

Telescopes and Instrumentation. **9151**, 271-287 (2014).

29. Jacobs, S.D. et al.Magnetorheological finishing: a deterministic process for optics manufacturing.International conference on optical fabrication and testing. **2576**, 372-382 (1995).

30. Comley, P. et al. Grinding metre scale mirror segments for the E-ELT ground based telescope. **60**, 379-382 (2011).

31. Yu, G., Walker, D.D. & Li, H.Research on fabrication of mirror segments for E-ELT.6th International Symposium on Advanced Optical Manufacturing and Testing Technologies: Advanced Optical Manufacturing Technologies. **8416**, 19-24 (2012).

32. Nee, A.Y.C. Handbook of manufacturing engineering and technology (Springer Publishing Company, Incorporated, 2014).

33. Yu, G. et al. Research on edge-control methods in CNC polishing. **13**, 24 (2017).

34. Hu, H. et al. Rapid fabrication strategy for Ø1. 5 m off-axis parabolic parts using computer-controlled optical surfacing. **57**, F37-F43 (2018).

35. Frapolli, C. et al.Key challenges for the production of ELT M1 segments at Safran Reosc.SPIE Astronomical Telescopes + Instrumentation. **12188**, 135-147 (2022).

36. Frapolli, C. et al.Radius of curvature matching for the Extremely Large Telescope M1.Advances in Optical and Mechanical Technologies for Telescopes and Instrumentation VI. **13100**, 180-190 (2024).

37. Zhang, P. et al. Application and development of bonnet polishing technology. **63**, 100901-100901 (2024).

38. Cayrel, M.J.G.-b. & IV, a.t. E-ELT optomechanics: overview. **8444**, 674-691 (2012).

39. Lawson, J. et al. Specification of optical components using the power spectral density function (SPIE, 1995).

40. Duparré, A. et al. Surface characterization techniques for determining the

root-mean-square roughness and power spectral densities of optical components. Applied Optics **41**, 154-171 (2002).

41. Cayrel, M. E-ELT optomechanics: overview (SPIE, 2012).

42. Randi, J.A., Lambropoulos, J.C. & Jacobs, S.D. Subsurface damage in some single crystalline optical materials. Applied Optics **44**, 2241-2249 (2005).

43. Cole, G.C. et al.An overview of optical fabrication of the JWST mirror segments at Tinsley.SPIE Astronomical Telescopes + Instrumentation. **6265**, 253-261 (2006).

44. Ji, P. et al. Towards a better understanding of the surface smoothing effect in gas cluster ion beam processing with molecular dynamics simulation and experiment. Optics Express **32**, 31965-31983 (2024).

45. Du, C. et al. High precision fabrication of aluminum optics by optimizing an Ar+ ion beam figuring strategy for polishing the contamination layer. Optics Express **29**, 28886-28900 (2021).

46. Oh, C.J. et al.Fabrication and testing of 4.2 m off-axis aspheric primary mirror of Daniel K. Inouye Solar Telescope.SPIE Astronomical Telescopes + Instrumentation. **9912**, 210-221 (2016).

47. Martin, H. et al.Manufacture of a combined primary and tertiary mirror for the Large Synoptic Survey Telescope.SPIE Astronomical Telescopes + Instrumentation. **7018**, 143-154 (2008).

48. Golini, D., Jacobs, Stephen D Physics of loose abrasive microgrinding. Applied Optics **30**, 2761-2777 (1991).

49. Dong, Z., Cheng, H.J.I.J.o.M.T. & Manufacture. Study on removal mechanism and removal characters for SiC and fused silica by fixed abrasive diamond pellets. **85**, 1-13 (2014).

50. Trumper, I. et al. Optics technology for large-aperture space telescopes: from fabrication to final acceptance tests. **10**, 644-702 (2018).

51. Suratwala, T. et al. Towards predicting removal rate and surface roughness during grinding of optical materials. **58**, 2490-2499 (2019).

52. Pilbratt, G.L. et al. Herschel Space Observatory-An ESA facility for far-infrared and submillimetre astronomy. Astronomy & Astrophysics **518**, L1 (2010).

53. Sein, E. et al.A 3.5 m diameter SiC telescope for Herschel mission.Astronomical Telescopes and Instrumentation. **4850**, 606-618 (2003).

54. Toulemont, Y. et al.The 3.5-m all-SiC telescope for HERSCHEL.SPIE Astronomical Telescopes + Instrumentation. **5487**, 1119-1128 (2004).

55. Yi, L. et al. Equivalent thin-plate method for stressed mirror polishing of an off-axis aspheric silicon carbide lightweight mirror. Optics Express **28**, 36413-36431 (2020).

56. Yi, L. et al. Comprehensive study of the rapid stressed mirror polishing method for off-axis aspheric SiC thin-plate mirrors. Optics Express **28**, 32802-32818 (2020).

57. Martin, H.M. et al.Active supports and force optimization for the MMT primary mirror.Astronomical Telescopes and Instrumentation. **3352**, 412-423 (1998).

58. Martin, H.M. et al.Fabrication of mirrors for the Magellan Telescopes and the Large Binocular Telescope.Astronomical Telescopes and Instrumentation. **4837**, 609-618 (2003).

59. Parodi, G., Hill, J. & Salinari, P.Supporting the 8.4 m honeycomb mirrors of Columbus.Progress in Telescope and Instrumentation Technologies, ESO Conference and Workshop Proceedings, ESO Conference on Progress in Telescope and Instrumentation Technologies, ESO, Garching, 27-30 April 1992, Garching: European Southern Observatory (ESO), 1992, edited by Marie-Helene Ulrich, p. 301. **42**, 301 (1992).

60. West, S.C. et al. Practical design and performance of the stressed-lap polishing tool. Applied Optics **33**, 8094-8100 (1994).

61. Bernstein, R. et al.Overview and status of the Giant Magellan Telescope project.SPIE Astronomical Telescopes + Instrumentation. **9145**, 494-509 (2014).

62. Bifano, T., Dow, T.A. & Scattergood, R.Microgrinding Optical Materials.Optical Fabrication and Testing. WC3 (1988).

63. Angel, J.R.P. & Parks, R.E.Lapping & Polishing with an Actively Stressed Lap.Workshop on Optical Fabrication and Testing. ThDA4 (1984).

64. Negi, V.S. et al. Challenges in the Fabrication of Off-Axis Mirror. (2021).

65. Zhao, H. et al. Deformation verification and surface improvement of active stressed lap for 4 m-class primary mirror fabrication. Applied Optics **54**, 2658-2664 (2015).

66. Bifano, T.G., Dow, T.A. & Scattergood, R.O.J.J.o.E.f.I. Ductile-Regime Grinding: A New Technology for Machining Brittle Materials. **113**, 184-189 (1991).

67. Martin, H.M. et al.Stressed-lap Polishing of Large, Highly Aspheric Primary Mirrors.Optical Fabrication and Testing Workshop. ThA5 (1992).

68. Tzordanidi, G. et al. Statistical model of metal removal removed from product surface under the influence of abrasive particle flow. (2020).

69. Martin, H.M.J.O. & News, P. Aspheric polishing with a stressed lap. **1**, 22-24 (1990).

70. Pileri, D. & Krabbendam, V.L.Hobby-Eberly primary mirror fabrication.SPIE's 1995 International Symposium on Optical Science, Engineering, and Instrumentation. **2536**, 344-349 (1995).

71. Jacobus, G.M. et al.Southern African Large Telescope (SALT) project: progress and status after two years.Astronomical Telescopes and Instrumentation. **4837**, 11-25 (2003).

72. Semenov, A.P. et al.Fabrication of blanks, figuring, polishing, and testing of segmented astronomic mirrors for SALT and LAMOST projects.SPIE Astronomical Telescopes + Instrumentation. **5494**, 31-38 (2004).

73. Nelson, J. The Keck Telescope: a new technology substitutes electronics for steel. American Scientist **77**, 170-176 (1989).

74. Mast, T.S. & Nelson, J.E.Fabrication of the Keck ten meter telescope primary

mirror.1985 Albuquerque Conferences on Optics. **542**, 48-59 (1985).

75. Martin, H. et al.Fabrication and testing of the first 8.4-m off-axis segment for the Giant Magellan Telescope.SPIE Astronomical Telescopes + Instrumentation. **7739**, 84-96 (2010).

76. Krabbendam, V.L. et al.Development and performance of Hobby-Eberly Telescope 11-m segmented mirror.Astronomical Telescopes and Instrumentation. **3352**, 436-445 (1998).

77. Martin, H.M. et al.Manufacture of primary mirror segments for the Giant Magellan Telescope.SPIE Astronomical Telescopes + Instrumentation. **10706**, 236-245 (2018).

78. Fan, C. et al. Local material removal model considering the tool posture in deterministic polishing. 0954406215598800 (2015).

79. Smith, B.K., Burge, J.H. & Martin, H.M.Fabrication of the 1.2 m Secondary Mirror for the Sloan Digital Sky Survey.Optical Fabrication and Testing. OFD.5 (1996).

80. Martin, H.M. et al.Manufacture and final tests of the LSST monolithic primary/tertiary mirror.SPIE Astronomical Telescopes + Instrumentation. **9912**, 278-294 (2016).

81. Jones, R.A. Fabrication of a large, thin, off-axis aspheric mirror. Optical Engineering **33**, 4067-4075 (1994).

82. Martin, H. et al.Manufacture of the second 8.4 m primary mirror for the Large Binocular Telescope.SPIE Astronomical Telescopes + Instrumentation. **6273**, 99-108 (2006).

83. Harris, D.C.History of magnetorheological finishing.SPIE Defense, Security, and Sensing. **8016**, 206-227 (2011).

84. Li, L.,Study on the key techniques of magnetorheological finishing for large aspheric optics[Changchun: Changchun Institute of Optics, Fine Mechanics and Physics, Chinese Academy of Sciences,2016.

85. Chen, S., Weng, Y. & Yao, B. Material removal model for magnetorheological

polishing considering shear thinning and experimental verification. Materials Today Communications **38**, 108475 (2024).

86. Lu, M.-M. et al. Research progress of magnetorheological polishing technology: a review. Advances in Manufacturing **12**, 642-678 (2024).

87. Zhao, C. et al. Improving detection accuracy of extreme-few-pixel Shack-Hartmann wavefront sensor based on tilt modulation. Optics Communications **570**, 130884 (2024).

88. Li, L. et al. Positive dwell time algorithm with minimum equal extra material removal in deterministic optical surfacing technology. Applied Optics **56**, 9098-9104 (2017).

89. Hull, T. et al.Lightweight high-performance 1-4 meter class spaceborne mirrors: emerging technology for demanding spaceborne requirements.SPIE Astronomical Telescopes + Instrumentation. **7739**, 104-117 (2010).

90. Li, L. et al. Rapid fabrication of a lightweight 2 m reaction-bonded SiC aspherical mirror. . Results Phys **10**, 903–912 (2018).

91. Bai, Y. et al. Rapid fabrication of a silicon modification layer on silicon carbide substrate. Applied Optics **55**, 5814-5820 (2016).

92. Liu, S. et al. Combined processing strategy based on magnetorheological finishing for monocrystalline silicon x-ray mirrors. Applied Optics **61**, 5575-5584 (2022).

93. Zhang, W. et al. Design of arrayed magnetorheological equipment applied in optics manufacture. Optics & Laser Technology **158**, 108892 (2023).

94. Guo, J. et al. Material removal mechanism and MR fluid for magnetorheological finishing of an RSA-6061 aluminum alloy mirror. Applied Optics **61**, 10098-10104 (2022).

95. Li, Y. et al. Evolution mechanism of scratch removal based on the implementation of magnetorheological finishing. Optics Express **32**, 11241-11258 (2024).

96. Bai, Y. et al. High precision polishing of aluminum alloy mirrors through a

combination of magnetorheological finishing and chemical mechanical polishing. Optics Express **32**, 15813-15826 (2024).

97. Tian, Y. et al. Combined polishing process of a sapphire aspherical component based on temperature-controlled magnetorheological processing. Applied Optics **62**, 805-812 (2023).

98. Lin, Z. et al. Prediction of surface roughness and the material removal rate in magnetorheological finishing. Optics Express **30**, 46157-46169 (2022).

99. Liu, X. et al. Tool mark prediction on the surface of large-aperture mirrors via magnetorheological finishing. Optics Express **32**, 11150-11170 (2024).

100. Chen, C. et al. Study on the influence of a magnetorheological finishing path on the mid-frequency errors of optical element surfaces. Optics Express **32**, 19133-19145 (2024).

101. Xu, M. et al. Investigation of surface characteristics evolution and laser damage performance of fused silica during ion-beam sputtering. Optical Materials **58**, 151-157 (2016).

102. Gressler, W.J. et al.LSST secondary mirror assembly.SPIE Astronomical Telescopes + Instrumentation. **10700**, 371-396 (2018).

103. Cui, X.Progress and prospect of LAMOST project.SPIE Astronomical Telescopes + Instrumentation. **6267**, 22-29 (2006).

104. Smith, G.M.Keck II status report.Optical Telescopes of Today and Tomorrow. **2871**, 10-14 (1997).

105. Burge, J.H. et al.Design and analysis for interferometric measurements of the GMT primary mirror segments.SPIE Astronomical Telescopes + Instrumentation. **6273**, 176-187 (2006).

106. Tuell, M. et al.Data processing for fabrication of GMT primary segments: raw data to final surface maps.SPIE Astronomical Telescopes + Instrumentation. **9151**, 1286-1297 (2014).

107. Geyl, R., Cayrel, M. & Tarreau, M.Gran Telescopio Canarias optics manufacture: progress report no. 2.Optical Systems Design. **5252**, 63-68 (2003).

108. Geyl, R., Cayrel, M. & Tarreau, M.Gran Telescopio Canarias optics manufacture: progress report no. 3.SPIE Astronomical Telescopes + Instrumentation. **5494**, 57-61 (2004).

109. Geyl, R. et al.First steps in ELT optics polishing.Fifth European Seminar on Precision Optics Manufacturing. **10829**, 16-25 (2018).

110. Jedamzik, R., Werner, T. & Westerhoff, T.Production of the world's largest convex ZERODUR mirror blank for the ELT.SPIE Astronomical Telescopes + Instrumentation. **11445**, 369-380 (2020).

111. Tonnellier, X. et al.Surface error correction of ELT primary mirror hexagonal segments by ion figuring.SPIE Astronomical Telescopes + Instrumentation. **13100**, 1160-1164 (2024).

112. Tozzi, A. et al. Toward ARIEL's primary mirror. 193 (2022).

113. Tozzi, A. et al.Toward ARIEL's primary mirror.Space Telescopes and Instrumentation 2022: Optical, Infrared, and Millimeter Wave. **12180**, 1518-1532 (2022).

114. Araiza-Durán, J.A. et al. Hartmann test using a screen with arbitrarily positioned holes. Applied Optics **63**, 5338-5345 (2024).

115. D'Anca, F. et al.Development, manufacturing, and testing of Ariel's structural model prototype flexure hinges.SPIE Astronomical Telescopes + Instrumentation. **13092**, 1485-1496 (2024).

116. Pace, E. et al.The telescope assembly of the Ariel space mission: an updated overview.SPIE Astronomical Telescopes + Instrumentation. **13092**, 419-429 (2024).

117. Burgett, W.S. et al. The Giant Magellan Telescope project in 2024: status and look ahead. 45 (2024).

118. Martin, H. et al.Production of 8.4 m primary mirror segments for GMT.Advances in Optical and Mechanical Technologies for Telescopes and Instrumentation V. **12188**, 177-184 (2022).

119. Walker, D. et al.The role of robotics in computer controlled polishing of

large and small optics.Optical Manufacturing and Testing Xi. **9575**, 50-58 (2015).

120. Pan, R. et al. Research on an evaluation model for the working stiffness of a robot-assisted bonnet polishing system. **65**, 134-143 (2021).

121. Li, L. et al.New generation magnetorheological finishing polishing machines using robot arm.AOPC 2019: Space Optics, Telescopes, and Instrumentation. **11341**, 315-318 (2019).

122. Cheng, R. et al. Accurately predicting the tool influence function to achieve high-precision magnetorheological finishing using robots. **31**, 34917-34936 (2023).

123. Invernizzi, A. et al.ELT secondary mirror manufacturing progress at Safran Reosc.Advances in Optical and Mechanical Technologies for Telescopes and Instrumentation IV. **11451**, 81-94 (2020).

124. Gu, P. et al. A grinding force prediction model for SiCp/Al composite based on single-abrasive-grain grinding. The International Journal of Advanced Manufacturing Technology **109**, 1563-1581 (2020).

125. Wang, S. et al. Ultra-precision raster grinding biconical optics with a novel profile error compensation technique based on on-machine measurement and wavelet decomposition. Journal of Manufacturing Processes **67**, 128-140 (2021).

126. Shanmugam, P., Lambropoulos, J.C. & Davies, M.A. Grinding of silicon carbide for optical surface fabrication, Part 1: surface analysis. Applied Optics **61**, 4579-4590 (2022).

127. Shanmugam, P., Lambropoulos, J.C. & Davies, M.A. Grinding of silicon carbide for optical surface fabrication. Part II. Subsurface damage. Applied Optics **62**, 3788-3796 (2023).

128. Sun, Z. et al. Ultra-precision time-controlled grinding for flat mechanical parts with weak stiffness. Journal of Manufacturing Processes **99**, 105-120 (2023).

129. Wang, S. et al. Evaluation of grinding characteristics for sapphire ultra-precision grinding using small grit sizes wheels based on AE signals. Journal of Manufacturing Processes **90**, 94-110 (2023).

130. Gu, P. et al. An error compensation method for single point oblique axis grinding considering the grinding wheel wear. Journal of Manufacturing Processes **112**, 32-44 (2024).

131. Sun, G. et al. Material removal and surface generation mechanisms in rotary ultrasonic vibration–assisted aspheric grinding of glass ceramics. The International Journal of Advanced Manufacturing Technology **130**, 3721-3740 (2024).

132. Wei, Q. et al. Ultra-precision milling and grinding for large-sagittal MgF2 aspheric optical elements. The International Journal of Advanced Manufacturing Technology **131**, 2985-3004 (2024).

133. Echerfaoui, Y., El Ouafi, A. & Sattarpanah Karganroudi, S. Dynamic errors compensation of high-speed coordinate measuring machines using ANN-based predictive modeling. The International Journal of Advanced Manufacturing Technology **122**, 2745-2759 (2022).

134. Mohammadi, F., Mirhashemi, M. & Rashidzadeh, R. A coordinate measuring machine with error compensation in feature measurement: model development and experimental verification. The International Journal of Advanced Manufacturing Technology, 1-11 (2022).

135. Moona, G. et al. Measurement uncertainty assessment of articulated arm coordinate measuring machine for length measurement errors using Monte Carlo simulation. The International Journal of Advanced Manufacturing Technology **119**, 5903-5916 (2022).

136. Song, M. et al. Calibration method of articulated arm coordinate measuring machine based on virtual calibrators. The International Journal of Advanced Manufacturing Technology **139**, 6343-6353 (2025).

137. Geyl, R., Cayrel, M. & Tarreau, M.Gran telescopio canarias optics manufacture.SPIE Astronomical Telescopes + Instrumentation. **6273**, 56-61 (2006).

138. Dierickx, P. et al.VLT primary mirrors: mirror production and measured

performance.Optical Telescopes of Today and Tomorrow. **2871**, 385-392 (1997).

139. Bacouel, A. et al.Hexagonal cutting for ELT M1.SPIE Astronomical Telescopes + Instrumentation. **13100**, 1102-1111 (2024).

140. Liang, Z.J. et al. Advances in research and applications of optical aspheric surface metrology. Chin. Opt **15**, 161-186 (2022).

141. Anderson, D.S. & Burge, J.H.Swing-arm profilometry of aspherics.SPIE's 1995 International Symposium on Optical Science, Engineering, and Instrumentation. **2536**, 169-179 (1995).

142. Zhu, R.H., Sun, Y. & Shen, H. Progress and prospect of optical freeform surface measurement. Acta Optica Sinica **41**, 0112001 (2021).

143. Oh, C.J. et al.Modern technologies of fabrication and testing of large convex secondary mirrors.SPIE Astronomical Telescopes + Instrumentation. **9912**, 238-249 (2016).

144. Anugu, N., Garcia, P.J.V. & Correia, C.M. Peak-locking centroid bias in Shack–Hartmann wavefront sensing. Monthly Notices of the Royal Astronomical Society **476**, 300-306 (2018).

145. Xiong, L.,Research on Swing Arm profilometer test for large-aperture complex optical surface[D],Changchun Institute of Optics, Fine Mechanics and Physics, University of Chinese Academy of Sciences,2017.

146. Berlakovich, N. et al. Fast modal reconstruction of large plane wavefronts from sparse measurements using Shack–Hartmann sensors. Applied Optics **62**, 6986-6992 (2023).

147. He, C. et al. A theoretical and deep learning hybrid model for predicting surface roughness of diamond-turned polycrystalline materials. International Journal of Extreme Manufacturing **5**, 035102 (2023).

148. Zhang, L. et al. Optical free-form surfaces testing technologies. Chinese Optics **10**, 283-299 (2017).

149. Häusler, G. et al.Deflectometry vs. interferometry.SPIE Optical Metrology 2013. **8788**, 367-377 (2013).

150. Knauer, M.C., Kaminski, J. & Hausler, G.Phase measuring deflectometry: a new approach to measure specular free-form surfaces.Photonics Europe. **5457**, 366-376 (2004).

151. Su, P. et al. Software configurable optical test system: a computerized reverse Hartmann test. Applied Optics **49**, 4404-4412 (2010).

152. Su, P. et al. Aspheric and freeform surfaces metrology with software configurable optical test system: a computerized reverse Hartmann test. Optical Engineering **53**, 031305-031305 (2014).

153. Zheng, Y. et al.Fringe projection-based single-shot 3d eye tracking using deep learning and computer graphics.SPIE AR | VR | MR. **12449**, 265-275 (2023).

154. Shen, M. et al. Deep learning based measurement accuracy improvement of high dynamic range objects in fringe projection profilometry. Optics Express **32**, 35689-35702 (2024).

155. Zhang, K. et al. Single-frame two-stage fringe projection profilometry based on deep learning. Applied Optics **64**, 855-865 (2025).

156. Li, J. et al. Dual-biprism-based coaxial fringe projection system. Applied Optics **61**, 3957-3964 (2022).

157. Zhang, X. et al. Phase retrieval from single-shot square wave fringe based on image denoising using deep learning. Applied Optics **63**, 1160-1169 (2024).

158. Di, R. et al. Lossless background encoding and phase-difference labeling used in fringe projection profilometry for high-precision three-dimensional reconstruction. Optics & Laser Technology **189**, 113021 (2025).

159. Yu, H. et al. Accurate defocusing fringe projection profilometry in a large depth-of-field. Optics & Laser Technology **164**, 109542 (2023).

160. Chen, M. et al.Recent developments of multi-aperture overlap-scanning technique.Optical Science and Technology, SPIE's 48th Annual Meeting. **5180**, 393-401 (2003).

161. Righini, G.C. & Consortini, A.J.P.o.S.-T.I.S.f.O.E. 19th Congress of the International Commission for Optics: Optics for the Quality of Life. (2003).

162. Wang, X.-k. et al.Test of an off-axis asphere by subaperture stitching interferometry.AOMATT 2008 - 4th International Symposium on Advanced Optical Manufacturing. **7283**, 518-523 (2009).

163. Chen, W. et al. Null test of large convex aspheres by subaperture stitching with replaceable holograms. Optics Communications **466**, 125665 (2020).

164. Cho, M., Liang, M. & Neill, D.Performance prediction of the LSST secondary mirror.SPIE Optical Engineering + Applications. **7424**, 47-57 (2009).

165. Burge, J.H., Su, P. & Zhao, C.Optical metrology for very large convex aspheres.SPIE Astronomical Telescopes + Instrumentation. **7018**, 421-432 (2008).

166. Mercier-Ythier, R. et al.Development of an interferometric test bench for the manufacturing of the ELT secondary mirror.SPIE Optical Systems Design. **13021**, 96-109 (2024).

167. Kim, G. et al. Dual subaperture stitching for large flat mirror testing. Applied Optics **59**, 8681-8687 (2020).

168. Pan, F. et al. Stitching sub-aperture in digital holography based on machine learning. Optics Express **28**, 6537-6551 (2020).

169. Wang, R. et al. Subaperture stitching interferometry based on the combination of the phase correlation and iterative gradient methods. Applied Optics **59**, 4176-4182 (2020).

170. Stašík, M. et al. Subaperture stitching computation time optimization using a system of linear equations. Applied Optics **60**, 8556-8568 (2021).

171. Wu, Q. et al. Simulation and measurement of systematic errors of stitching interferometry for high precision X-ray mirrors with large radius of curvature. Applied Optics **60**, 8694-8705 (2021).

172. Lan, M. et al. Measurement of aspheric mirrors using arc-region scanning and data stitching technology. The International Journal of Advanced Manufacturing Technology **121**, 6035-6048 (2022).

173. Wang, S. et al. Scanning strategy for surface defects evaluation of large fine optical components. Optics & Laser Technology **156**, 108473 (2022).

174. Wu, Q. et al. Mixed stitching interferometry with correction from one-dimensional profile measurements for high-precision X-ray mirrors. Optics Express **31**, 16330-16347 (2023).

175. Yang, Z. et al. Automatic measurement system for large-aperture-angle non-holonomic spherical stitching with laser differential confocal interference. Applied Optics **63**, 699-707 (2024).

176. Sun, Y. et al. Research on Coherent Stray Light Fringes in Interference Compensation Testing. Photonics **11**, 74 (2024).

177. Stryjewski, E., Zielinski, R. & Smith, J.Testing The Primary Mirror of the W. M. Keck Observatory.30th Annual Technical Symposium. **0680**, 54-58 (1987).

178. Mast, T.S. & Nelson, J.E.Fabrication of large optical surfaces using a combination of polishing and mirror bending.SPIE Astronomical Telescopes and Instrumentation for the 21st Century. **1236**, 670-681 (1990).

179. Peter, L.W. et al.Optical quality of the W.M. Keck Telescope.1994 Symposium on Astronomical Telescopes and Instrumentation for the 21st Century. **2199**, 94-104 (1994).

180. Malacara, D. Optical shop testing (John Wiley & Sons, 2007).

181. Wu, F. Design of Dall compensator for aspherical surface null testing. Journal of Applied Optics **14**, 1-4 (1993).

182. Offner, A. A Null Corrector for Paraboloidal Mirrors. Applied Optics **2**, 153-155 (1963).

183. Lucian, A.M.Test And Evaluation Of The Hubble Space Telescope 2.4-meter Primary Mirror.29th Annual Technical Symposium. **0571**, 182-190 (1986).

184. Christopher, J.B.Hubble Space Telescope optics: problems and solutions.Orlando '91. **1494**, 528-533 (1991).

185. McLure, R.J., Dunlop, J.S. & Kukula, M.J. Two-dimensional modelling of optical Hubble Space Telescope and infrared tip-tilt images of quasar host galaxies. Monthly Notices of the Royal Astronomical Society **318**, 693-702 (2000).

186. Park, Y., Casertano, S. & Ferguson, H.C. Optimal Galaxy Shape Measurements for Weak Lensing Applications Using the Hubble Space Telescope Advanced Camera for Surveys. The Astrophysical Journal **600**, L159 (2004).

187. Roland, G. & Marc, C.REOSC contribution to VLT and Gemini.Optical Systems Design and Production. **3739**, 40-46 (1999).

188. Cayrel, M. et al.Gemini 8.2-m primary mirror no. 1 polishing.Astronomical Telescopes and Instrumentation. **3352**, 205-215 (1998).

189. Mountain, C.M., Gillett, F. & Oschmann, J.Gemini 8-m telescopes.Astronomical Telescopes and Instrumentation. **3352**, 2-13 (1998).

190. Tu, S.H.I. et al. Surface testing methods of aspheric optical elements. Chinese Optics **7**, 26-46 (2014).

191. Guo, P., Yu, J. & Shun, X. Null lens design for small aspherical surface with large NA. Optics and Precision Engineering **10**, 518-522 (2002).

192. Ono, A. & Wyant, J.C. Aspherical mirror testing using a CGH with small errors. Applied Optics **24**, 560-563 (1985).

193. Beyerlein, M., Lindlein, N. & Schwider, J. Dual-wave-front computer-generated holograms for quasi-absolute testing of aspherics. Applied Optics **41**, 2440-2447 (2002).

194. Kurita, M. et al. The Seimei telescope project and technical developments. Publications of the Astronomical Society of Japan **72**, 48 (2020).

195. Wang, X. et al. Concave aspheric test combining Dall with Offner null compensation using a plane wave. Applied Optics **59**, 8987-8996 (2020).

196. Ye, L. et al. Testing of large-aperture aspheric mirrors using a single coated lens. Applied Optics **59**, 4577-4582 (2020).

197. de Groot, P.J. et al. Contributions of holography to the advancement of interferometric measurements of surface topography. Light: Advanced Manufacturing **3**, 258-277 (2022).

198. Hao, S. et al. Mapping distortion correction in off-axis aspheric mirror testing with a null compensator. Applied Optics **61**, 4040-4046 (2022).

199. Beisswanger, R., Pruss, C. & Reichelt, S. Retrace error calibration for interferometric measurements using an unknown optical system. Optics Express **31**, 27761-27775 (2023).

200. Qiao, X. et al. Absolute testing of optical flats using minimum norm least squares solutions. Optics Express **32**, 37260-37269 (2024).

201. Xu, K. et al. Accuracy verification methodology for computer-generated hologram used for testing a 3.5-meter mirror based on an equivalent element. Light: Advanced Manufacturing **5**, 195-203 (2024).

202. Kino, M., Kurita, Mikio Interferometric testing for off-axis aspherical mirrors with computer-generated holograms. %J Applied optics **51**, 4291-4297 (2012).

203. Chaney, D., Hadaway, J. & Lewis, J.Cryogenic radius of curvature matching for the JWST primary mirror segments.SPIE Optical Engineering + Applications. **7439**, 336-344 (2009).

204. Whitman, T. et al.Alignment test results of the JWST Pathfinder Telescope mirrors in the cryogenic environment.SPIE Astronomical Telescopes + Instrumentation. **9904**, 1381-1388 (2016).

205. Hadaway, J.B. et al.Performance of the primary mirror center-of-curvature optical metrology system during cryogenic testing of the JWST Pathfinder telescope.Space Telescopes and Instrumentation 2016: Optical, Infrared, and Millimeter Wave. **9904**, 1445-1454 (2016).

206. Shore, P. & Parr-Burman, P.Manufacture of large mirrors for ELTs: a fresh perspective.Optical Systems Design. **5252**, 55-62 (2004).

207. Mercier-Ythier, R. et al.The interferometric test bench for ELT M2: the largest convex precision mirror ever made.SPIE Astronomical Telescopes + Instrumentation. **13100**, 380-393 (2024).

208. Sporer, S.F.TMT: stressed mirror polishing fixture study.SPIE Astronomical Telescopes + Instrumentation. **6267**, 961-973 (2006).

209. McElwain, M.W. et al. The James Webb Space Telescope Mission:

optical telescope element design, development, and performance. Publications of the Astronomical Society of the Pacific **135**, 058001 (2023).

210. Zhou, P. & Burge, J.H. Optimal design of computer-generated holograms to minimize sensitivity to fabrication errors. Optics Express **15**, 15410-15417 (2007).

211. Chen, M.-y. et al. Neural network based surface shape modeling of stressed lap optical polishing. Applied Optics **49**, 1350-1354 (2010).

212. Buchnev, O. et al. Deep-Learning-Assisted Focused Ion Beam Nanofabrication. Nano Letters **22**, 2734-2739 (2022).

213. Yan, K. et al. Mapping model of ribbon contour and tool influence function based on distributed parallel neural networks in magneto-rheological finishing. Optics Express **32**, 27099-27111 (2024).

214. Wang, R. et al. Material removal rate optimization with bayesian optimized differential evolution based on deep learning in robotic polishing. Journal of Manufacturing Systems **78**, 178-186 (2025).

215. Zha, Z. et al. Deep learning physical hybrid model-driven in situ cutting force monitoring of ultra-precision diamond turning. Measurement Science and Technology **36**, 096120 (2025).

216. Zhang, Z. et al. Intelligent modeling and detection in grinding: a review of advances, challenges, and prospects. The International Journal of Advanced Manufacturing Technology **138**, 4995-5055 (2025).

217. Lu, X. et al. Prediction of three-dimensional coordinate measurement of space points based on BP neural network. International Journal of Manufacturing Research **15**, 218-233 (2020).

218. Fan, L. et al. Deep learning-based Phase Measuring Deflectometry for single-shot 3D shape measurement and defect detection of specular objects. Optics Express **30**, 26504-26518 (2022).

219. Chang, X. et al. Dynamic Interferometry for Freeform Surface Measurement Based on Machine Learning-Configured Deformable Mirror. Sensors

25, 490 (2025).

220. Reyna, M.A.J. et al. Calibration of wavefront aberrations using supervised learning and deep learning for a Shack–Hartmann wavefront sensor. Optical Engineering **64**, 053101 (2025).

221. Yu, X. et al. On the use of deep learning for computer-generated holography. iScience **28**, 112507 (2025).

222. Zhang, Z. et al. Fringe-Based Structured-Light 3D Reconstruction: Principles, Projection Technologies, and Deep Learning Integration. Sensors **25**, 6296 (2025).